Multiple Roles for *Saccharomyces cerevisiae* Histone H2A in Telomere Position Effect, Spt Phenotypes and Double-Strand-Break Repair

Holly R. Wyatt,* Hungjiun Liaw,† George R. Green‡ and Arthur J. Lustig*,†,[1]

**Interdisciplinary Program in Molecular and Cellular Biology and* †*Department of Biochemistry, Tulane University Health Sciences Center, New Orleans, Louisiana 70112 and* ‡*Department of Pharmaceutical Sciences, Southern School of Pharmacy, Mercer University, Atlanta, Georgia 31207*

Manuscript received August 21, 2002
Accepted for publication January 13, 2003

ABSTRACT

Telomere position effects on transcription (TPE, or telomeric silencing) are nucleated by association of nonhistone silencing factors with the telomere and propagated in subtelomeric regions through association of silencing factors with the specifically modified histones H3 and H4. However, the function of histone H2A in TPE is unknown. We found that deletion of either the amino or the carboxyltails of H2A substantially reduces TPE. We identified four H2A modification sites necessary for wild-type efficiency of TPE. These "*hta1tpe*" alleles also act as suppressors of a δ insertion allele of *LYS2*, suggesting shared elements of chromatin structure at both loci. Interestingly, we observed combinatorial effects of allele pairs, suggesting both interdependent acetylation and deacetylation events in the amino-terminal tail and a regulatory circuit between multiple phosphorylated residues in the carboxyl-terminal tail. Decreases in silencing and viability are observed in most *hta1tpe* alleles after treatment with low and high concentrations, respectively, of bleomycin, which forms double-strand breaks (DSBs). In the absence of the DSB and telomere-binding protein yKu70, the bleomycin sensitivity of *hta1tpe* alleles is further enhanced. We also provide data suggesting the presence of a yKu-dependent histone H2A function in TPE. These data indicate that the amino- and carboxyl-terminal tails of H2A are essential for wild-type levels of yKu-mediated TPE and DSB repair.

GENES positioned adjacent to a telomere are epigenetically repressed, or silenced, a phenomenon known as telomere position effect (TPE; Gottschling *et al.* 1990). TPE has been observed in organisms ranging from yeast to humans (Baur *et al.* 2001). In yeast, TPE is a metastable process in which repressed and derepressed states are each maintained for multiple generations (Gottschling *et al.* 1990; Monson *et al.* 1997; Enomoto and Berman 1998; Park and Lustig 2000). Under these conditions, dense, specifically positioned nucleosomes are coupled with multiple associations among nonhistone regulatory proteins in subtelomeric chromatin to form a closed structure, similar to the transcriptionally quiescent heterochromatin of higher eukaryotes (Gottschling *et al.* 1990; Gottschling 1992; Wright *et al.* 1992; Venditti *et al.* 1999).

The genetic regulation of telomeric silencing bears striking similarities to silencing of the cryptic mating-type loci located close to the left (*HMLα*) and right (*HMRa*) telomeres of chromosome III (Lustig 1998). The telomere contains a subset of factors and *cis*-acting sequences that act at the *HM* loci. Silencing is initiated within the telomere by the recruitment of the nonhistone chromatin proteins Sir2, Sir3, and Sir4 by the yKu70/yKu80 heterodimer and Rap1, the major telomeric binding protein that is highly conserved through evolution (Cockell *et al.* 1998a; Gasser and Cockell 2001; Luo *et al.* 2002). This recruitment is coupled with associations among Sir factors, including Sir3/Sir4, Sir3/Sir3, and Sir2/Sir4, that extend into subtelomeric regions (Laroche *et al.* 1998; Gasser and Cockell 2001; Moazed 2001; Hoppe *et al.* 2002; Luo *et al.* 2002). In addition, the Sir proteins associate with additional nonhistone proteins, including Dot4 (Kahana and Gottschling 1999), Sif1 (Cockell *et al.* 1998b), and Ubp3 (Moazed and Johnson 1996).

Subsequent unidirectional spreading of the subtelomeric heterochromatic state (Renauld *et al.* 1993) requires a multiplicity of proteins, including the NAD-dependent histone deacetylase Sir2. This deacetylase targets specific lysine residues within both histone H4 (K16) and histone H3 (K14) (Imai *et al.* 2000; Landry *et al.* 2000; Moazed 2001; Suka *et al.* 2001; Carmen *et al.* 2002). In addition, interactions of both Sir3 and Sir4 with histones H3 and H4 are required for telomeric silencing (Hecht *et al.* 1995; Lustig 1998; Carmen *et al.* 2002). As in other organisms, recent evidence has also implicated Set1-mediated histone H3 methylation

[1]*Corresponding author:* Department of Biochemistry SL-43, Tulane University Health Sciences Center, 1430 Tulane Ave., New Orleans, LA 70112. E-mail: alustig@tulane.edu

activity in yeast heterochromatin formation (Briggs *et al.* 2001; Lachner *et al.* 2001; Krogan *et al.* 2002).

The formation of highly condensed "silenced" chromatin states also involves the interaction of telomeric and subtelomeric bound Rap1 and Sir factors. This interaction may be mediated through a "hairpin" looped structure or less-defined interactions within telomeric sequences (Grunstein 1998; de Bruin *et al.* 2000, 2001; Park and Lustig 2000).

Previous studies have indicated that the N-terminal tail of histone H2A is required for repression of basal transcription (Lenfant *et al.* 1996; Recht *et al.* 1996). In addition, truncation of the amino terminus results in an inability to grow on different carbon sources such as raffinose and galactose (Hirschhorn *et al.* 1995). In contrast, phosphorylation within the carboxyl-terminal region of H2A has been linked, among other processes, to replication, DNA damage, and histone deposition (Green and Poccia 1989; Downs *et al.* 2000; Green 2001; Ward and Chen 2001; Redon *et al.* 2002). While an extensive body of data supports the involvement of the amino termini of histones H3 and H4 in telomeric silencing, the role of H2A in telomere position effects has remained uncertain (Grunstein 1998).

Like other histones, H2A has a long, positively charged amino terminus (operationally defined as between amino acids 1–20) that extends outside the nucleosome space (Luger and Richmond 1998). However, histone H2A is unique in that its carboxyl-terminal region (defined here as residues 120–131) also extends into the extranucleosomal space (Luger *et al.* 1997; Luger and Richmond 1998). This latter region exits the nucleosome between DNA gyres as they wrap around the histone octamer, near the dyad axis, leaving the carboxyl-terminal tails poised to influence access of nucleosomal DNA to regulatory factors. Both extended termini contain multiple potentially modified residues that could regulate the heterochromatin-like subtelomeric structure, possibly by mediating interactions with specific silencing proteins.

Mutations or reductions in the abundance of H2A and H2B confer suppression of auxotrophy caused by insertion of δ, the Ty1 long terminal repeat, into either upstream activation or 5′ coding regions of genes such as *HIS4* and *LYS2*, termed an Spt$^-$ (*s*u*p*pressor of *T*y1) phenotype. (Clark-Adams and Winston 1987; Clark-Adams *et al.* 1988; Swanson *et al.* 1991). Wild-type and *lys2-128*δ cells initiate transcription at the *LYS2* promoter; however, the *lys2-128*δ allele creates an early stop codon that results in a short inactive protein. In contrast, in *spt* mutant cells, the δ promoter is functional, leading to a slightly shorter, but active, gene product (Swanson *et al.* 1991). These Spt$^-$ phenotypes may be the consequence of alterations in the transcriptional initiation (or elongation; see below) mediated through alterations in chromatin structure (Hartzog *et al.* 1998; Yamaguchi *et al.* 2001). Consistent with this, *spt11* and *spt12* are alleles of *HTA1* and *HTB1*, respectively (Clark-Adams *et al.* 1988).

Mutations in *SPT4*, *SPT5*, and *SPT6* interact genetically with the amino-terminal tails of histone H2A and H2B fusion proteins to confer transcriptional repression when either histone is tethered adjacent to a reporter gene (Recht *et al.* 1996). Furthermore, overproduction of H2A and H2B can suppress the phenotypes of mutations in several *SPT* genes (Sherwood and Osley 1991). The stage at which these gene products act in transcription is not fully resolved, although more recent evidence suggests a role for these proteins in the elongation of transcripts through specific chromatin states (Hartzog *et al.* 1998; Yamaguchi *et al.* 2001; Pokholok *et al.* 2002). This view is consistent with studies from Gross' lab suggesting that silencing is likely to be the consequence of defects in Pol II elongation rather than in accessibility of the template (Sekinger and Gross 2001).

In this study, we investigated the role of histone H2A in telomeric silencing. We find that specific alleles of histone H2A, but not H2B, substantially reduce TPE (collectively termed the *hta1tpe* alleles). Deletion mutations of either the amino or the carboxyl tails produced significant reductions in TPE efficiency. A site-directed mutational analysis of modifiable sites in H2A led to the identification of residues in both amino- and carboxyl-terminal tails that influence TPE efficiency, implicating specific sites of acetylation and phosphorylation as functionally important. Furthermore, all *hta1tpe* point mutations also confer a strong Spt$^-$ phenotype.

Interestingly, we find that the silencing defects of *hta1tpe* alleles are exacerbated by bleomycin-induced double-strand-break (DSB) formation. Furthermore, we find that the TPE defects in *hta1tpe* alleles are more severe in the absence of yKu70 function. H2A is intrinsically involved in yKu-mediated silencing. Many of the *hta1tpe* alleles increased the sensitivity to bleomycin and displayed a heightened requirement for yKu70 in DSB repair. These data suggest a mechanistic link between repair of bleomycin-induced DSBs and H2A involvement in the regulation of telomeric, subtelomeric, and Spt$^+$ chromatin structure.

MATERIALS AND METHODS

Plasmids: pJH55 is a pRS313 derivative that carries the genomic *Bam*HI-*Sac*II fragment of the *HTA1-HTB1* locus as the sole source of histones H2A and H2B. Plasmid pJH55 and its derivatives carrying *hta1* mutations Δ*4-20* (Δ*N*), *S19P*, *S19F*, *K21E*, Δ*120-131* (Δ*C*), and *S121P* have been previously described (Hirschhorn *et al.* 1995). Plasmids containing the *hta1* alleles *K4R/K7R*, *K4M/K7M*, *K7R*, *K13R*, and *K13M* were the kind gift of Barbara Dunn and Mary Ann Osley. Derivatives of pRS314 carrying the *htb1* deletion mutations (Δ*3-32*, Δ*3-22*, Δ*14-31*) were previously described (Recht and Osley 1999). *Eco*RI-*Bam*HI fragments of these plasmids carrying the mutant *hta1/HTB1* locus were cloned into pRS313. Additional point mutations in the H2A coding region (*S1A*, Δ*N/S1A*, *K4R*, *K21M*, *K21R*, *S121A*, *T125A*, *T125E*, *S128A*, *S128E*, and the

double mutants *T125A/S128A* and *T125E/S128E*) were constructed via site-directed mutagenesis of pJH55 (Stratagene, La Jolla, CA). The *S128A* mutation was created two times with no difference in phenotype. Mutant plasmids were sequenced to verify the presence of each mutation using flanking primers. Bacterial culture and transformations were performed according to standard procedures.

Yeast strains and media: Rich (YPD or YPAD), synthetic complete (SC), and fluoroorotic acid (FOA)-containing SC media (SC + FOA) were prepared according to standard procedures. All strains used in this study were derived from FY406 [*MAT***a** (*hta1-htb1*)Δ::*LEU2* (*hta2-htb2*)Δ::*TRP1* his3Δ*200 trp1*Δ*63 lys2-128*δ *ura3-52 leu2*Δ*1* pSAB6], an S288C derivative, which carries the sole source of H2A and H2B on pSAB6 (Hirschhorn *et al.* 1995). A plasmid shuffle was used to replace the wild-type pSBA6 with wild-type or mutant pJH55 derivatives. pSBA6 loss was selected on the basis of resistance to FOA and verified by Southern analysis. Growth rates for each strain were determined in liquid YPAD media at 30°.

pRS306 vectors containing *URA3* sequences were linearized using either *Nco*I or *Stu*I and subsequently transformed into FY406 or *hta1* mutants. Since these restriction sites lie upstream of the Ty insertion site of *ura3-52*, within the *URA3* coding region, the resulting integrant contains the wild-type *URA3* gene adjacent to the genomic *ura3-52* allele.

The *yku70* null alleles were generated by targeted PCR. *yku70::kan*^{r} were amplified by PCR from BY4741/*yku70::kan*^{r} (*MAT***a** *yku70::kan*^{r} *his3*Δ*1 leu2*Δ*0 met15*Δ*0 ura3*Δ*0*; Winzeler *et al.* 1999; ATCC) using two primers, 5′-T AGACGGACTCA TAATTGAATGGTT-3′ and 5′-CACTTGGCGTGGTTTATTAGA CTAT-3′, corresponding to upstream and downstream sequences of *YKU70*, respectively. The PCR product was transformed into strains containing the wild-type, Δ*N*, and *T125A* alleles. *YKU70* disruptions were verified by both PCR and Southern analysis. Additionally, each of the *yku70* strains was temperature sensitive at 37° and produced short telomeres, as expected.

Silencing and fluctuation analyses: V_R or VII_L telomeres were labeled with *URA3* as previously described (Gottschling *et al.* 1990). Telomere labeling was verified by Southern analysis. Telomere length was not affected by the introduction of any *hta1* mutation tested in this study (data not shown). Telomeric silencing was measured using fluctuation analysis (Liu *et al.* 1994). Briefly, cells containing either *URA3*-marked-VII_L or -V_R telomeres were streaked onto rich medium and grown for 3–4 days at 30°. Seven colonies of ~1.5 mm in diameter were selected, appropriately diluted, and plated onto SC and SC + FOA plates. Colonies were counted after 3 days of growth at 30° and 7 additional days of growth at room temperature. The data were analyzed for statistical significance relative to wild type both by determination of 95% confidence limits around the mean and by the rank-sum test from at least three independent fluctuation analyses. Significant changes determined by the 95% confidence limits were also significant by the rank-sum test in all silencing assays.

To determine the effect of γ-irradiation exposure on TPE in the *hta1tpe* alleles, fluctuation analyses were conducted as described above, except that cells plated on SC and SC + FOA plates were immediately exposed to 20 Gy irradiation (~70% viability).

During the course of these studies we found that sensitivity of Ura3$^-$ cells on SC + FOA + bleomycin (SC+ FOA+ bleo) plates is increased relative to growth on SC+ bleo (data not shown). We therefore first determined the percentage viability of Ura3$^-$ cells in each *hta1* mutant relative to wild type at the same dosage of bleomycin, represented by [($FOA^r_{xbleo/hta1}$/$FOA^r_{xbleo/HTA1}$) × 100], where *x* is the concentration of bleomycin. The percentage values represent the sensitivity of cells to bleomycin on SC + FOA plates. The results did not qualitatively differ from sensitivity to bleomycin on SC plates lacking FOA (data not shown).

To discern the quantitative effect of bleomycin on TPE, 1.5-mm colonies were dispersed in 300 μl ddH_2O and plated in 5- to 10-fold dilutions onto SC + FOA plates, as indicated. The first lane corresponded to a 5-μl aliquot of a 1:10 dilution of the initial cell suspension. Initial (silencing + sensitivity) values in cells containing a *URA3*-marked VIIL telomere were obtained relative to wild type at the same bleomycin dose, as described above, and are equal to [($FOA^r_{xbleo/hta1/URA3\text{-}VIIL}$/$FOA^r_{xbleo/HTA1/URA3\text{-}VIIL}$) × 100]. To take into account bleomycin killing at the same dose and mutant, we normalized the values as [($FOA^r_{xbleo/hta1}$/$FOA_{xbleo/hta1/URA3/VIIL}$)] for each dose. To determine the loss of silencing due to increasing doses of bleomycin in a single mutant, the values are normalized to the 0 bleomycin control. The loss of silencing is then described by [($FOA^r_{xbleo/hta1}$/$FOA_{xbleo/hta1/URA3\text{-}VIIL}$)/($FOA^r_{0\ bleo/hta1}$/$FOA^r_{0bleo/hta1/URA3\text{-}VIIL}$)].

The effect of *yku70* in wild-type and *hta1tpe* cells was calculated by comparing the ratios [FOA^r (*HTA1 YKU70*)/FOA^r (*HTA1 yku70*)] to [FOA^r (*hta1tpeYKU70*)/FOA^r (*hta1tpe yku70*)]. Chi-square analysis, where each value is the sum of five multiple trials, was used to determine the significance of differences between these ratios. Quantitative mating-type tests for *HML*α silencing were conducted as previously described (Kyrion *et al.* 1993).

Spt$^-$ quantification: Suppression of *lys2-128*δ was assayed by the ability of cells to grow on lysine omission media. Following growth on YPD or YPAD media, 1.5- to 2.0-mm colonies were dispersed into 300 μl ddH_2O and 10-fold serial dilutions were prepared. A total of 25 μl of a 10^{-3} dilution and a 10^{-2}–10^0 dilution were plated onto SC and SC-lysine omission media, respectively. Colonies were counted after growth at 25° for 6 days. The mean for each mutant was determined after multiple trials (more than three trials) and is presented as [(SC-lysine colonies)/(SC colonies) × 100] ± 95% confidence limits.

γ-Irradiation resistance: Colonies of 1.5 mm were selected after growth on YPAD and dispersed into 10-fold serial dilutions of a 300-μl ddH_2O suspension. For 0–20 Gy exposure, we plated 25 μl of a 10^{-3} dilution. For 200 Gy exposure, 25–50 μl of a 10^{-2} dilution were plated. Plating was conducted in duplicate to synthetic complete media and immediately exposed to varying levels of γ-irradiation in a Cs-137 irradiation chamber. Cells were grown at 30° for 3 days postexposure and 7 additional days at room temperature before colony counts and survival ratios were determined. Resistance data were evaluated as the mean survival ratio as defined by [(number of colonies on γ-exposed plates/number of colonies on unexposed plates) ± the 95% confidence limits] for at least three independent experiments.

Plasmid end-joining assays: Cells were transformed with 1 μg of *Sac*I-linearized pRS316, releasing a 4-bp overhang, and plated in duplicate for selection on SC-Ura (uracil omission) plates. Dilutions of each transformation were also plated in duplicate on SC plates to control for plating efficiency. Final colony counts were made after 6 days of growth at 30°. The number of successful transformation events was determined as (number of colonies on SC-Ura/number of colonies on SC plates). For all alleles, each transformation was normalized to its wild-type control and the mean values were determined together with the 95% confidence intervals. Circular pRS316 transformation efficiencies were originally used as transformation controls. However, circular and linear efficiencies appear not to be correlated with respect to DNA concentration, apparently due to different optimum transformation efficiencies for linear *vs.* circular DNA.

Histone quantification: *Chromatin isolation:* Yeast cells were

grown in 60 ml YPAD with continuous shaking at 25°. Cultures were inoculated with cells from a stationary overnight culture and were grown to mid-log phase (OD at 600 nm = 0.3). Cells were collected by centrifugation (2000 × *g* for 5 min) and the two cell pellets obtained from each culture were combined by suspension in 30 ml YPAD. The washed cells were collected by centrifugation as described above. The cell pellet was chilled on ice to 4° and mixed with 1.5 ml chromatin isolation buffer [CIB; 0.15 M NaCl, 10 mM Tris-Cl, pH 8.0, 0.5% Triton X-100, 1 mM β-mercaptoethanol, 1 mM sodium butyrate, 10 mM NaFl, 1 mM $NaVO_3$, 0.1 mM phenylmethylsulfonyl fluoride (PMSF), pH 8.0]. All subsequent steps were conducted at 4°. Glass beads were added to the top of the liquid surface and the capped tube was vortexed for 1 min. A total of 30 ml CIB was added to the tube and the contents were thoroughly mixed. The glass beads were allowed to settle and the supernatant was decanted into a fresh centrifuge tube. The glass beads were washed with 5 ml CIB, which were combined with the supernatant. Insoluble material, including the yeast chromatin, was recovered by centrifugation (20,000 × *g* for 5 min). The pellet was then suspended in 30 ml chromatin wash buffer (CWB; 0.15 M NaCl, 10 mM Tris-Cl, pH 8.0, 1 mM β-mercaptoethanol, 1 mM sodium butyrate, 10 mM NaFl, 1 mM $NaVO_3$, 0.1 mM PMSF, pH 8.0) and insoluble material was collected by centrifugation. When analyzed for steady-state histone phosphorylation, stationary overnight cultures were inoculated and incubated in the presence of 1.0 mCi $^{32}PO_4$ (New England Nuclear) and allowed to develop to logarithmic growth before collection.

Histone extraction: To extract histones, the washed chromatin pellet was suspended in 1 ml CWB supplemented with 10 μl protamine sulfate (10 mg/ml; Sigma Type X). The suspended chromatin was mixed with 1 ml 0.4 M H_2SO_4 and incubated for 24 hr with occasional mixing. Acid insoluble material was pelleted by centrifugation at 14,000 × *g* for 10 min and the supernatant was mixed with 1/4 volume 100% trichloroacetic acid and incubated on ice for 1 hr. Precipitated histones were collected by centrifugation at 14,000 × *g* for 10 min and the pellet was suspended in cold acetone containing 0.1% H_2SO_4. The washed histones were collected by centrifugation (14,000 × *g* for 5 min), washed with cold acetone, and dried at room temperature. Purified histones were dissolved in 100 μl acid urea loading buffer (5% acetic acid, 8 M urea, 5% β-mercaptoethanol, 0.01% crystal violet) and analyzed by two-dimensional polyacrylamide gel electrophoresis, as previously described (Green *et al.* 1990). The ^{32}P-histone steady-state labeling patterns of histones were determined by phosphoimager scanning with quantitative software (Image Gauge V3.3). The stoichiometry of histones after Coomassie blue staining of two-dimensional gels was determined after scanning using Image Gauge software.

RESULTS

Deletion of the amino or carboxyl tails of histone H2A reduces the efficiency of TPE: The essential roles of the amino-terminal tails of histone H3 and H4 in yeast silencing have been extensively documented (Grunstein 1998). However, far less is known about the potential TPE functions of the highly conserved amino-terminal and highly variant carboxyl-terminal tails of histone H2A (Thompson *et al.* 1994; Green 2001). To study the effects of mutations in the amino- and carboxyl-terminal tail of H2A, we used a strain in which one of the two copies of *HTA-HTB* (*HTA2-HTB2*) was deleted and the second *HTA1-HTB1* locus was present on a centromeric plasmid (Hirschhorn *et al.* 1995). The strains also contained a *URA3*-marked telomere at the left arm of chromosome VII (VII_L) and, in some mutants, at the right arm of chromosome V (V_R; Gottschling *et al.* 1990). The silencing of the *URA3* gene was assayed by the ability to grow in the presence of 5-FOA (FOA^R), which allows the growth of $Ura3^-$, but not of $Ura3^+$, cells. Significant differences were determined by nonoverlapping 95% confidence limits and rank-sum tests.

We first examined yeast strains containing amino-terminal deletions of *H2A1* or *H2B1* and a *URA3*-marked VII_L telomere. In strains carrying a deletion of amino acids 4–20 (Δ*N*) of H2A, FOA^R colonies decreased from the wild-type mean of 0.20 to the Δ*N* value of 0.01 (Figure 1 and Figure 2A). Furthermore, the Δ*N* deletion in cells carrying the *URA3*-marked V_R telomere decreased silencing >40-fold to the limit of detection ($m = <$ 0.000053, Figure 2B). The Δ*N* TPE phenotype was identical to TPE in *S1A/*Δ*N* double mutants, which eliminates all amino-terminal sites of modification (Figure 2A). In contrast, although the amino terminus of H2B plays a role in chromatin-mediated transcriptional repression (Recht *et al.* 1996), a series of analogous *H2B* amino-terminal deletion mutants conferred wild-type levels of silencing, consistent with the results of a previous study (Thompson *et al.* 1994; Figure 1). Hence, the amino-terminal TPE phenotypes are a unique property of the *hta1* alleles.

Similarly, deletion of amino acids 120–131 (ΔC) of *H2A1* resulted in a significant (3-fold) mean decrease in silencing at the VII_L telomere (27.8 ± 2.8%) with an unusually broad 36-fold range of values surrounding the median. A more severe (10-fold) effect was observed at the *URA3*-marked V_R telomere (Figure 2B). These results indicate that both the amino and carboxyl termini of histone H2A are necessary for wild-type levels of telomeric silencing.

A role for regulated aminoterminal acetylation and deacetylation in TPE: Previous biochemical studies have led to the identification of modifiable residues within the H2A amino terminus, some of which may influence TPE. In the amino terminus, two of these sites, K4 and K7, can be acetylated (Ohba *et al.* 1999; White *et al.* 1999; Vogelauer *et al.* 2000; Suka *et al.* 2001; Goll and Bestor 2002). Simultaneous mutation of both of these lysine residues to arginine (*K4R/K7R*) significantly reduces silencing at both the *URA3*-VII_L (3-fold) and V_R (20-fold) marked telomeres (Figure 2, A and B). In contrast, mutations that mimic the charge of an acetylated state (*K4M/K7M*) had a slightly enhanced TPE phenotype, consistent with a role for histone H2A acetylation in TPE (27 ± 2.8%). However, no amino-terminal single mutation of a lysine to arginine (*K4R*, *K7R*, *K13R*, *K21R*; Figure 2A) confers a reduction in TPE. Consistent with the known deacetylation of K7 in heterochromatin (Suka *et al.* 2001), K7R hyper-represses TPE at both V_R and VII_L telomeres (Figure 2, A and B),

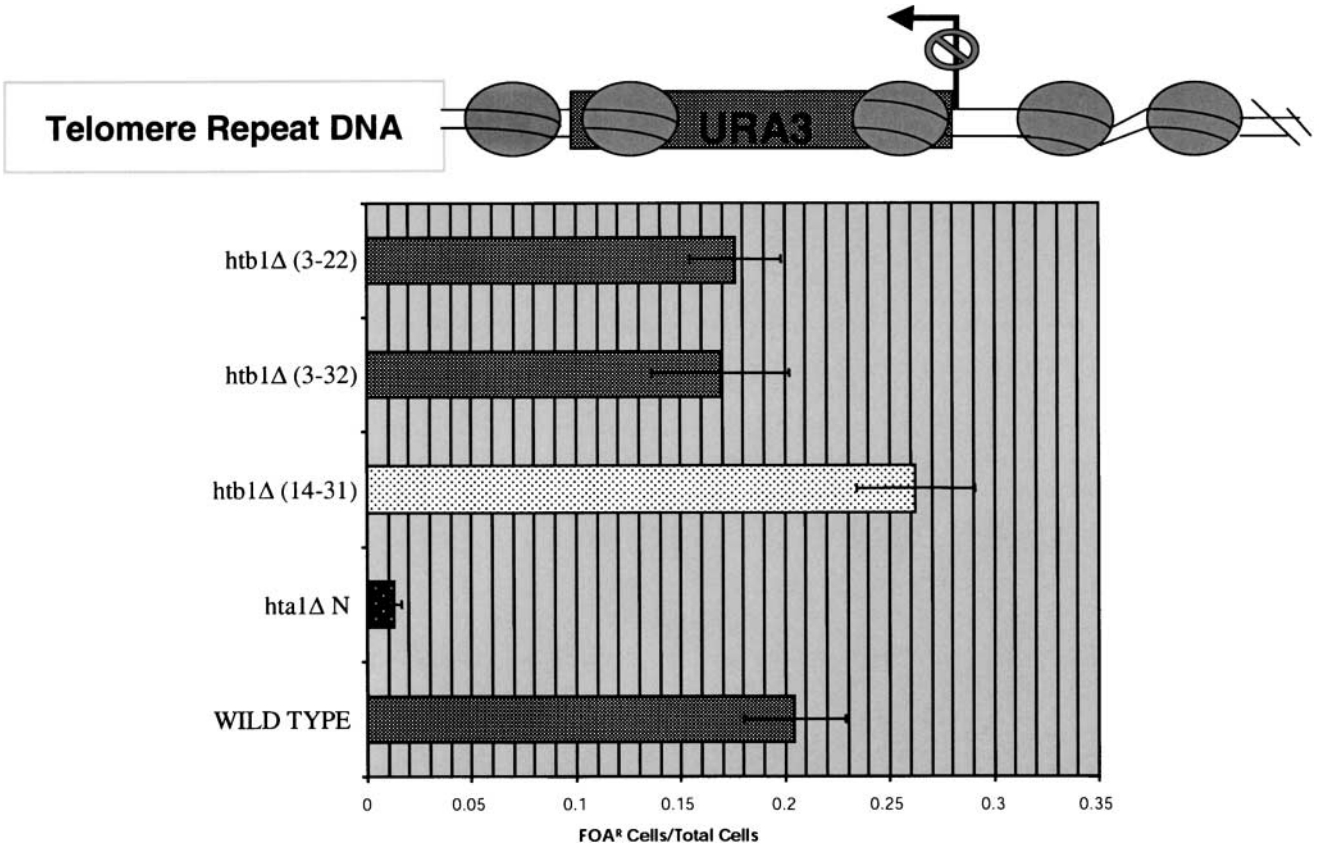

FIGURE 1.—The *HTA1* N-terminal tail functions in TPE. (Top) Representation of a *URA3*-marked VII_L telomere. Arrow, direction of *URA3* transcription; ovals, subtelomeric nucleosomes; stop mark, silencing of the *URA3* gene. (Bottom) Seven FY406 colonies containing plasmid-encoded wild-type H2A and H2B [t (number of trials) = 3, n (pooled sample size) = 21], *hta1*Δ*(4-20)[*Δ*N*] (t = 3, n = 21), *htb1*Δ*(14-31)* (t = 3, n = 21), *htb1*Δ*(3-31)* (t = 3, n = 21), or *htb1*Δ*(3-22)* (t = 3, n = 21) were dispersed, diluted, and spread onto individual SC or SC + FOA plates. Silencing was measured as the mean fraction of FOA-resistant cells from pooled data. Gray stippled bars represent mean values that are not statistically different from those of wild type; the white stippled bar represents mean values that are statistically higher than those of wild type; and the black stippled bar represents mean values that are significantly lower than those of wild type. Error brackets represent the 95% confidence intervals.

indicating that the *K4R/K7R* double mutant eliminates the hyper-repression observed in *K7R* cells. Hence, the *K4R/K7R* double mutant decreases silencing beyond the value for each single mutant, suggesting an antagonistic interaction between K4 and K7 residues in this microenvironment.

We obtained an additional effect on telomeric silencing after mutation of K21 located within the amino-terminal α-helical region (REDON *et al.* 2002). Altering the charge status of residues in this region could produce structural changes resulting in TPE sensitivities. Indeed, mutation of K21 to a neutral or basic charge conferred wild-type levels of silencing. In contrast, mutation of K21 to a negatively charged amino acid led to a modest, but significant, twofold decrease in silencing at the VII_L telomere (Figure 2A). These data raise the possibility that the α-helix may be a structural facilitator of telomeric silencing.

Multiple phosphorylation sites within the H2A carboxyl terminus: As noted above, deletion of the carboxyl-terminal 11 amino acids of histone H2A results in a reduction in telomeric silencing. Interestingly, this region contains three potential sites for phosphorylation: S121, T125, and S128. To test the possible modification of these residues, we analyzed the steady-state labeling of ^{32}P-labeled histones from different mutants by two-dimensional polyacrylamide gel electrophoresis. The phosphorylation of histone H2A was measured relative to a common nonhistone species. While deletion of the C terminus eliminated ~95% of all phosphorylation, single mutations in two of the three residues (T125A and S128A) did not decrease phosphorylation levels more than twofold (Table 1; Figure 3). Even the *T125A/S128A* allele did not result in loss of phosphorylation comparable to Δ*C* values, suggesting a role for S121 in C-terminal phosphorylation under specific conditions. This is consistent with our finding that the triple mutant *S121A/T125A/S128A* has growth rates (2.95 ± 0.25 hr) far slower than those for simple deletion of the C terminus (2.1 ± 0.14 hr) or growth of T125A/S128A mutants (1.71 ± 0.3 hr). Curiously, a single *S121A* mutation confers a major increase in H2A phosphorylation, suggesting upregula-

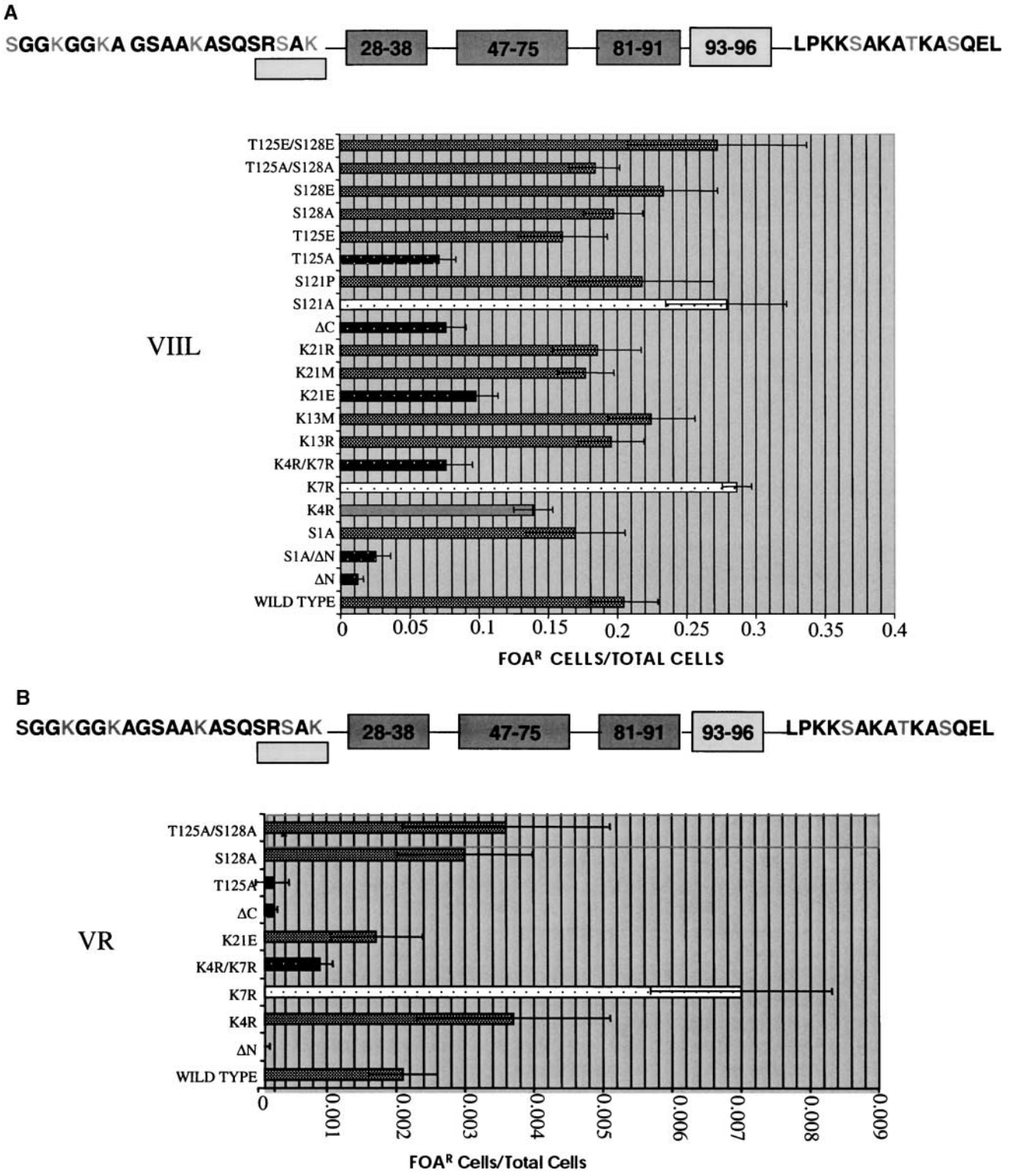

FIGURE 2.—(A) The identification of *hta1tpe* alleles. (Top) Representation of the amino- and carboxyl-tail domains of histone H2A1. All mutant residues tested are shaded. □, small α-helix; ■, histone fold domains. (Bottom) The silencing phenotype of FY406 cells at the *URA3*-marked VII_L telomere-containing plasmid-encoded wild-type *HTA1* ($t = 3$, $n = 21$), *hta1Δ(4-20)*[*ΔN*] ($t = 3$, $n = 21$), *hta1S1A/ΔN* ($t = 3$, $n = 21$), *hta1S1A* ($t = 3$, $n = 21$), *hta1K4R* ($t = 2$, $n = 14$), *hta1K7R* ($t = 3$, $n = 21$), *hta1K4R/K7R* ($t = 3$, $n = 21$), *hta1K13R* ($t = 4$, $n = 28$), *hta1K13M* ($t = 3$, $n = 21$), *hta1K21E* ($t = 3$, $n = 21$), *hta1K21R* ($t = 3$, $n = 21$), *hta1K21M* ($t = 3$, $n = 21$), *hta1Δ(121-131)*[*ΔC*] ($t = 12$, $n = 84$), *hta1S121A* ($t = 2$, $n = 14$), *hta1S121P* ($t = 3$, $n = 21$), *hta1T125A* ($t = 3$, $n = 21$), *hta1T125E* ($t = 2$, $n = 14$), *hta1S128A* ($t = 3$, $n = 21$), *hta1S128E* ($t = 2$, $n = 14$), *hta1T125A/S128A* ($t = 3$, $n = 21$), or *hta1T125E/S128E* ($t = 2$, $n = 14$) were determined as described in the legend for Figure 1. The additional alleles that were tested but had no effect on telomeric silencing were *K4MK7M, S19F,* and *S19P.* (B) The silencing phenotype of FY406 cells at the *URA3*-marked V_R telomere-containing plasmid-encoded wild-type *HTA1* ($t = 5$, $n = 35$), *hta1ΔN* ($t = 2$, $n = 14$), *hta1K4R* ($t = 2$, $n = 14$), *hta1K7R* ($t = 6$, $n = 42$), *hta1K4R/K7R* ($t = 3$, $n = 21$), *hta1K21E* ($t = 3$, $n = 21$), *hta1ΔC* ($t = 2$, $n = 14$), *hta1T125A* ($t = 2$, $n = 14$), *hta1S128A* ($t = 2$, $n = 14$), and *hta1T125A/S128A* ($t = 5$, $n = 35$) were conducted as described in the legend for Figure 1. Bar graphs, symbols, and error brackets (95% confidence limits) are defined as in the legend for Figure 1.

TABLE 1

Growth rate, abundance, and phosphorylation of *hta1* alleles

Mutant	Growth rate	%H2A/(H2A + H2B + H3 + H4)	γ*hta1/HTA1*[a] (%)
W303(WT)	1.58 ± 0.28 (3)	NT	NT
FY406(WT)	1.56 ± 0.15 (5)	19.5 ± 1.2 (3)	100
Δ*N*	1.89 ± 0.11 (4)	14.4 ± 2.9 (3)	82[b]
K4R, K7R	1.78 ± 0.60 (2)	NT	NT
K21E	1.54 ± 0.08 (5)	NT	NT
ΔC[c]	2.10 ± 0.08 (11)	14.6 ± 4.7 (3)	4.60
S121P	1.98 (1)	18.7 ± 2.3	569
T125A	1.64 ± 0.22 (3)	17.5 ± 2.8 (3)	44
S128A	1.71 ± 0.27 (4)	17.3 ± 2.3 (3)	72
T125A/S128A	1.71 ± 0.30 (4)	17.3 ± 1.0 (2)	30

NT, not tested.

[a] The qualitative pattern of results from this single representative experiment was replicated in subsequent experiments.

[b] This allele was tested only once within the context of this experiment.

[c] Underlined alleles represent significant changes in phosphorylation levels.

tion of phosphorylation at T125 and/or S128 residues. These data suggest that phosphorylation is distributed among multiple residues under non-DNA damage conditions and raises the possibility of regulated switching between phosphorylated residues.

The effect of phosphorylation site loss on TPE: To discern the possible function of these residues in TPE, we analyzed the effects of *hta1* mutants in each of the potential phosphorylation sites at S121 (S121A and S121P), T125 (T125A, T125E), and S128 (S128A, S128E). Mutations in only one of these three residues, T125A, led to a decrease in TPE at both marked telomeres. A 3-fold and >20-fold decrease was observed in the mean TPE frequencies at the *URA3*-marked VII_L and V_R telomeres, respectively (Figure 2).

If the negative charge produced by phosphorylation is the regulatory information supplied by this modification (Green 2001), then a mutation that mimics the negative charge of a phosphorylated residue should overcome the silencing defect produced by the *T125A* mutation. Accordingly, we found that, unlike *T125A*, *T125E* has no silencing defect. Similarly, silencing levels of neither the *S128A* nor the *S128E* allele differed from those of wild-type or *T125E* cells (Figure 2A), consistent with a requirement for a negative charge at T125 for wild-type levels of TPE.

Nonetheless, while S128A does not confer direct defects in telomeric silencing, S128 does appear to play a subtler role in TPE. Specifically, we have uncovered genetic interactions between residues S128 and T125. The presence of an S128A residue rescues the *T125A* TPE defect in *T125A/S128A* double mutants (Figure 2). These data suggest a regulatory circuit between T125 and S128 in the carboxyl-terminal microenvironment.

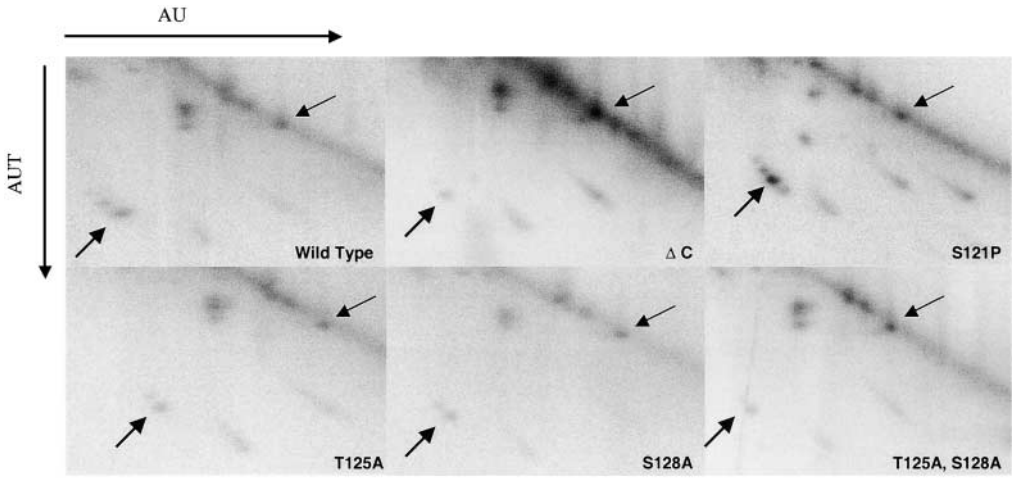

Figure 3.—A complex pattern of C-terminal hydroxylamino acid phosphorylation. Autoradiograms of two-dimensional polyacrylamide gels of ^{32}P-labeled histones isolated from FY406 cells containing plasmid-borne wild-type *HTA1*, *hta1*Δ*C*, *hta1S121P*, *hta1T125A*, *hta1S128A*, or *hta1T125A/S128A* are shown. The bottom arrow of each panel indicates the position of the H2A species as identified by previous staining of the gel with Coomassie blue. The upper arrow refers to the species used as a control. H2A protein spots migrating to the upper left of the major H2A proteins are acetylated and/or phosphorylated isoforms. Note that overexposure of the *hta1*ΔC autoradiogram is required to visualize the ^{32}P-labeled histone H2A. H2A histone proteins generated by the different deletion alleles display an alteration of electrophoretic mobility due to size and charge effects.

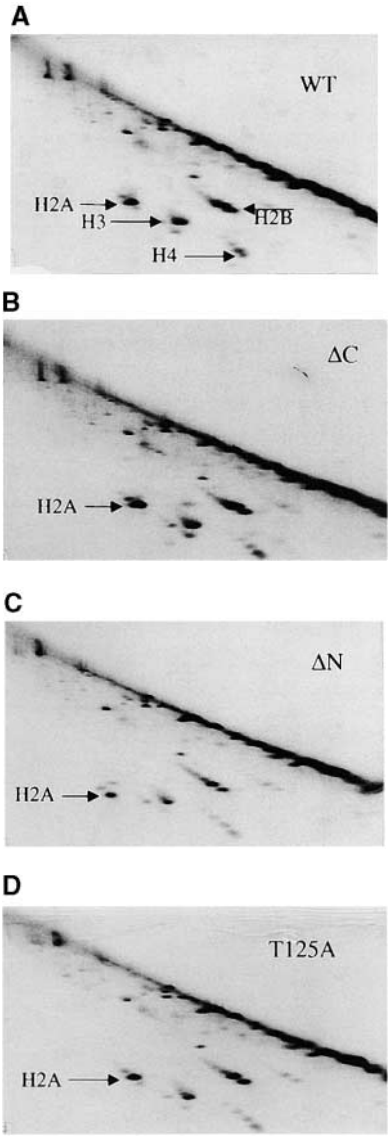

FIGURE 4.—Wild-type abundance of H2A in *hta1tpe* alleles. Coomassie-blue-stained two-dimensional polyacrylamide gels from independently isolated chromatin from FY406 cells containing a plasmid-borne wild-type *HTA1* (WT), *hta1*Δ*C*, *hta1*Δ*N*, and *hta1T125A*. Other alleles tested (but not shown here) are *hta1S121A*, *hta1T125A*, *hta1S128A*, and *hta1T125A/S128A*. In all cases the percentage [H2A/(H2A + H2B + H3 + H4)] was quantified. Values of this ratio did not vary among wild-type and *hta1tpe* alleles by >20%. Therefore, alterations in H2A abundance cannot account for the phenotypes observed in this study. The position of each histone is shown in A, and the arrows in B–D indicate the positions of H2A. Histone H2A proteins generated by Δ*N* and Δ*C* alleles have slightly altered relative positions on the gel.

Nonspecific effects of the *hta1tpe* alleles are unlikely to explain these phenotypes. First, in most mutants, doubling times do not differ from those in wild type, with the exception of Δ*N* and Δ*C* strains that grow slightly more slowly than wild type (Table 1). In the case of Δ*C*, this slower growth rate appears to be associated with the production of inviable or growth-arrested cells during culture (data not shown). However, growth rates do not correlate with the extent of silencing or any other phenotype assayed in this study (*cf.* Table 1 and Figure 2A). Second, two-dimensional gel electrophoresis of wild-type and mutant histones revealed that histone H2A did not exhibit significant differences in abundance, ruling out effects of underproduction or overproduction (Table 1; Figure 4). Third, a second sensitive telomere phenotype, telomere tract size, is not altered in any of the histone H2A alleles (data not shown).

The *hta1tpe1* alleles do not influence steady-state *HML* silencing: Yeast telomeric silencing and the cryptic mating-type silencing at the *HM* loci share common mechanistic elements. These include the histone H3 and H4 deacetylase Sir2 and the silencing proteins Sir3 and Sir4 that dock with the amino termini of both histone H3 and histone H4 in heterochromatic DNA (HECHT *et al.* 1995; MOAZED 2001; CARMEN *et al.* 2002). The expression levels of *HML*α in wild-type and *hta1tpe* alleles were assayed by a quantitative mating-type assay that can detect small shifts in silencing. We observed no changes in steady-state mating efficiencies of either Δ*N* (45 ± 3.4%) or Δ*C* mutants (58 ± 10%) or of any other *hta1tpe* allele tested relative to wild type (50 ± 6.3%; Table 2).

All *hta1tpe* alleles confer Spt⁻ phenotypes: Previous studies have shown that alterations in *HTA1* gene dosage can suppress the auxotrophy conferred by the insertion of δ into the *LYS2* 5′ coding region (CLARK-ADAMS *et al.* 1988; SHERWOOD and OSLEY 1991). The suppression or activation of δ-element transcriptional initiation or elongation has served as a classic model for the identification of factors involved in altering higher-order chromatin, including histones H2A and H2B (SHERWOOD and OSLEY 1991).

Interestingly, each *hta1tpe* allele confers Spt⁻ suppression of *lys2-128*δ, as indicated by the percentage of cells capable of forming a Lys⁺ colony (see Figure 5). The Spt⁻ phenotypes differed in their severity. Increases of 10- to 20-fold in Lys⁺ cells were exhibited by Δ*N*, Δ*C*, and *T125A/S128A hta1tpe* alleles (Figure 5B). In contrast, more dramatic 1000- to 2000-fold increases were observed for *hta1K4R/K7R*, *hta1K21E*, and *hta1T125A* missense mutations (Figure 5A). Hence, deletions of the amino or carboxyl termini confer phenotypes that differ significantly from mutations within the two tail regions. In contrast, neither *hta1S121A* nor *hta1S128A* alleles exhibited an Spt⁻ phenotype.

The two combinatorial effects observed for TPE values are maintained in the Spt⁻ cells. In the case of K4R and K7R, neither single mutant confers an Spt⁻ phenotype. In contrast, the Spt⁻ phenotype of the K4R/K7R double mutant is elevated 1000-fold over wild type. Similarly, T125A confers a 1000-fold increase in Spt⁻ cells, while S128A does not confer an Spt⁻ phenotype. The T125A/S128A allele retains only a 10-fold increase in Lys+ cells, far closer to the S128A than to the T125A phenotype (Figure 5). The common presence of these

TABLE 2

Summary of *hta1tpe* allele phenotypes

Mutation	Telomere position effects			*HML* silencing	*spt* suppression	Bleo^R	NHEJ
	VIIL	VIIL + Bleo	VR				
WT	+++	+++	+++	+++	−	+++	+++
Δ*N*	+	±	−	+++	++	±	++
K4R	+++	NT	+++	NT	−	NT	NT
K7R	++++	NT	++++	NT	−	+++	+++
K4R/K7R	++	+++	++	+++	++++	+++	+++
K21E	++	±, +++	+++	NT	++++	++	++
Δ*C*	++	+++	±	+++	++	±	+++
S121A/P	+++	NT	NT	+++	NS	NT	NT
T125A	++	+	±	+++	++++	+	++
S128A	+++	+++	+++	NT	−	+++	+++
T125A/S128A	+++	+++	+++	NT	−	+++	+++

+++, WT (20% FOA^r); ++, 2–10× < WT; +, 10–100× < WT; ±, 100–1000× < WT; ++++, >WT. *HML* silencing: WT (50% mating). *spt* suppression: −, basal wild-type values (5×10^{-3} Lys$^+$); ++, 0.02–0.1% Lys$^+$; ++++, 10–20% Lys$^+$. Bleomycin resistance at 15 mU/ml: +++, wild-type resistance (∼35% colony growth); ++, 2–10× < WT; +, 10–100× < WT; ±, 100–1000 < WT; plasmid endjoining: +++, wild type (2×10^{-5}); ++, 2–10 < WT; NS, not statistically significant; NT, not tested.

genetic interactions suggests a mechanistic relationship between loss of silencing with an increased severity of the Spt$^-$ phenotype.

Formation of bleomycin-induced DSBs further decreases silencing in *hta1tpe* alleles: Recent data have suggested the presence of an equilibrium of silencing and repair factors between the telomere and the sites of DSBs, leading to lower levels of silencing (Martin *et al.* 1999; McAinsh *et al.* 1999; Mills *et al.* 1999). If the defects of the *hta1tpe* alleles studied here are acting through the stability of telomeric chromatin structure, then these mutants may influence the loss of telomeric factors after DSB formation. One test of this hypothesis is the level of telomeric silencing during or after DNA damage. To test the effects of DNA damage formation on TPE, we grew cells in the presence of bleomycin. Bleomycin creates DSBs that use homologous recombination (at <20 mU/ml) and yKu-dependent nonhomologous endjoining (NHEJ) at higher doses (Mages *et al.* 1996; Milne *et al.* 1996; Martin *et al.* 1999; Mills *et al.* 1999; Moore *et al.* 2000).

The *hta1tpe* cells were grown in low doses (5 mU/ml) of bleomycin. Under these conditions, both mutant and wild-type cells display only a ∼2-fold decrease in viability (see materials and methods). A striking decrease in TPE was observed in most *hta1tpe* mutant cells (Figure 6). On the basis of FOA-resistant growth in the presence or absence of the marked telomere, the Δ*N* allele conferred a >800-fold decrease over the wild-type value containing no bleomycin. This decrease is >40-fold above that of mutant cells lacking bleomycin, leading to the formation of microcolonies on SC + FOA + bleo plates (Figure 6, A and B). *K21E* colonies generate two distinct phenotypes on SC + FOA plates that differ in their response to bleomycin treatment (population 1, $n = 2$; population 2, $n = 3$). The first phenotype did not respond to bleomycin at 5 mU/ml, while the second population displayed a 50-fold decrease in silencing compared to mutant cells lacking bleomycin (Figure 6). This variability may be the consequence of epigenetic switches between H2A states or differences in the plasmid copy number. In contrast to other alleles, the *K4R/K7R* mutation does not respond to DNA damage.

The Δ*C* allele did not give rise to a diminished TPE phenotype in response to DNA damage. In contrast, the *T125A* missense mutation within the carboxyl-terminal tail conferred a fivefold decrease in TPE in response to 5 mU/ml bleomycin. This defect is coupled with a concomitant decrease in growth rate compared to *T125A* cells grown in the absence of bleomycin. As in the absence of bleomycin, *T125A/S128A* did not confer a defect in silencing or in growth rate in the presence of bleomycin. Hence, the production of DSBs by bleomycin in most *hta1tpe* missense alleles exacerbated telomeric silencing.

Numerous studies have suggested that γ-irradiation is repaired in a yKu-independent mechanism, as is the nucleotide excision repairs following UV-induced damage (Moore 1989; Milne *et al.* 1996; Mills *et al.* 1999). Interestingly, cells treated transiently with γ-irradiation do not display a major TPE response to DNA damage. Only one of the *hta1tpe* alleles, *K21E*, conferred a fourfold decrease in TPE after irradiation ($m = 0.0252$) compared to nonirradiated cells. These data indicate that the *hta1tpe* response to DNA damage may be dependent on differing mechanisms of DNA repair, such as yKu-dependent and -independent NHEJ and homologous recombination.

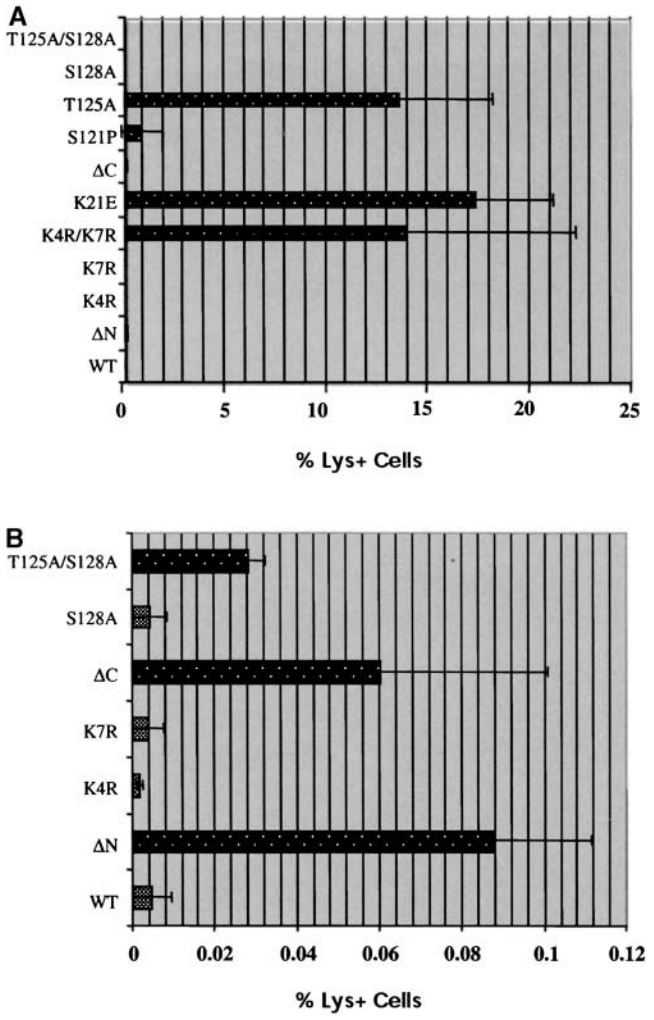

FIGURE 5.—All *hta1tpe* alleles confer Spt⁻ phenotypes. For each experiment, suppression was measured by counting the number of cells capable of growth on lysine omission media relative to total cells. The cells assayed were FY406 cells containing a plasmid-borne copy of wild-type *HTA1* ($n = 4$), *hta1ΔN* ($n = 4$), *hta1K4R* ($n = 3$), *hta1K7R* ($n = 3$), *hta1K4R/K7R* ($n = 4$), *hta1K21E* ($n = 4$), *hta1ΔC* ($n = 8$), *hta1S121P* ($n = 4$), *hta1T125A* ($n = 5$), *hta1S128A* ($n = 4$), and *hta1T125A/S128A* ($n = 3$). Mean values not statistically different from those of wild type are shown by gray stippled bars, while values higher than those of wild type are indicated by black stippled bars. Error brackets denote 95% confidence limits. All alleles are shown in A, while only lower-suppressing alleles are shown in B. Note that although the mean value of *hta1S121P* is relatively high, the large error precludes a conclusion regarding this allele.

A subset of *hta1tpe* mutants is hypersensitive to specific classes of DSBs: Growth on bleomycin destabilizes telomeric chromatin through the release of shared silencing/repair factors (*e.g.*, yKu heterodimer and Sir3) to other nuclear sites, including induced DSBs (MARTIN *et al.* 1999; MCAINSH *et al.* 1999; MILLS *et al.* 1999). This depletion leads to decreases in telomeric silencing in response to DNA damage, but does not explain the response of cell viability to bleomycin. In wild-type cells, we observe a twofold decrease in viability at 5 mU/ml and a sixfold decrease at 15 mU/ml, similar to previous reports (MARTIN *et al.* 1999; MCAINSH *et al.* 1999). The "telomere-release" model predicts that *hta1tpe* alleles should release additional competent DNA repair factors, resulting in a consequential increase in double-strand-break repair, realized as increased bleomycin resistance.

In striking contrast, our results suggest that the converse appears to be true. Differential sensitivity to bleomycin was observed in the range between 15 and 20 mU/ml bleomycin and, with the exception of *K4R/K7R*, followed the pattern of *hta1tpe* phenotypes (Figure 7). In the case of the Δ*N*, Δ*C*, and *T125A*, the viability of cells at 15 mU/ml was 450-, 200-, and 17-fold lower, respectively, than that of wild type. In addition, colony growth rates were decreased compared to wild-type cells. *S128A* and *T125A/S128A* behave identically to wild type, suggesting once again the dominance of the *S128A* phenotype over *T125A*. A qualitatively similar result was obtained after growth of cells on SC + FOA + bleo (Figure 7) or on SC + bleo (Figure 9A; data not shown). These observations suggest two possibilities: that the *hta1tpe* alleles are defective in both telomeric silencing and DSB repair or that the two phenotypes are both linked to a telomeric defect in response to bleomycin-specific DSBs (see DISCUSSION).

A second approach used to measure DNA repair in the presence of the *hta1tpe* mutants is an *in vivo* plasmid repair assay reflecting predominantly yKu-dependent repair (DOWNS *et al.* 2000; MATERIALS AND METHODS). Following plasmid cleavage with *Sac*I and transformation into wild-type or *hta1tpe* mutant cells, mean transformation efficiencies relative to wild type were determined (Figure 8). The products of plasmid rejoining were both simple ligations of the *Sac*I site and ligations in which the *Sac*I site was eliminated (data not shown). The eliminated sites are likely to reflect end degradation (or recombinational rearrangement) and religation (BOULTON and JACKSON 1998). With the exception of Δ*C*, all of the *hta1tpe* alleles that displayed bleomycin sensitivity also displayed defects (ranging from 25 to 50% of wild-type values) in the plasmid repair assay. Once again, *S128A* and the *T125A/S128A* double mutant displayed wild-type phenotypes. In this assay, Δ*C* conferred wild-type transformation levels. This allele may disjoin multiple pathways that process unique substrates through NHEJ or homologous recombination pathways. Consistent with this possibility we have found that the enhanced sensitivity to bleomycin in ΔC cells is not accompanied by an increase in yKu dependence (data not shown).

Genetic interactions between *hta1ΔN* and *hta1T125A* and the *yku70* pathways: The effects of bleomycin on TPE suggested that the *hta1tpe* alleles may more easily titrate the yKu heterodimer from telomeres to DSBs due to either an increased number of bleomycin-specific

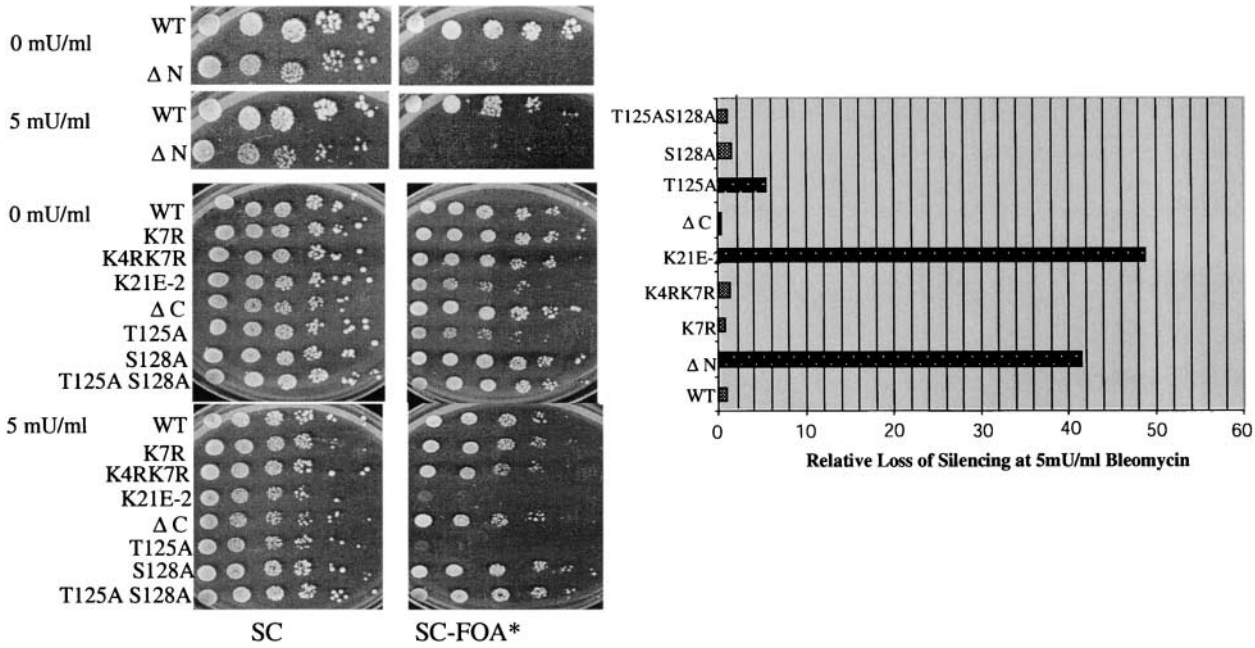

FIGURE 6.—*hta1tpe* silencing is further diminished after DNA DSB formation. (Left) To discern the effect of bleomycin on TPE, 1.5-mm colonies were dispersed in 300 μl ddH_2O and fivefold serial dilutions of FY406 strains containing wild-type *HTA1*, *hta1K7R*, *hta1K4R/K7R*, *hta1K21E-2*, *hta1ΔC*, *hta1T125A*, *hta1S128A*, and *hta1T125A/S128A* were plated onto SC or SC + FOA media containing either 0 or 5 mU/ml bleomycin. For SC plates, the first lane corresponds to 5-μl of a 1:50 dilution of the initial cell suspension. For SC + FOA plates, the first lane corresponds to a 5 μl aliquot of a 1:10 dilution of the initial cell suspension. Subsequent lanes represent fivefold serial dilutions in the presence or absence of 5 mU/ml bleomycin. Microcolonies are difficult to visualize in these photographs. (Right) To compensate for the increase of bleomycin sensitivity on SC + FOA, values for wild-type *HTA1* [*n* (number of trials) = 6], *hta1ΔN* (*n* = 4), *hta1K7R* (*n* = 4), *hta1K4R/K7R* [*n* (0 mU) = 4, *n* (5 mU) = 5], *hta1K21E* (*n* = 5), *hta1ΔC* (*n* = 6), *hta1T125A* (*n* = 6), *hta1S128A* (*n* = 6), and *hta1T125A/S128A* (*n* = 4) were normalized to wild type at 5 mU/ml of bleomycin in the presence or absence of a *URA3*-marked telomere. For each allele, the relative decrease in silencing was determined as described in MATERIALS AND METHODS. The resulting values are plotted in the graph. Gray stippled bars refer to values that do not statistically differ from wild type; black stippled bars represent >20-fold decreases in silencing relative to wild type. K21E-2 refers to one of two phenotypes that this allele displays on SC + FOA plates following induction of DNA damage.

DSB or an alteration in telomeric chromatin structure. We would therefore predict a greater dependence of DSB on the presence of yKu in *hta1tpe* alleles. To test this hypothesis, we assayed sensitivity to varying doses of bleomycin in wild-type, Δ*N*, and *T125A* alleles in the presence or absence of yKu70. The sensitivity of wild-type cells at 15 mU/ml bleomycin was 40–50% of the 0 mU/ml bleomycin value in both *YKU70* and *yku70*

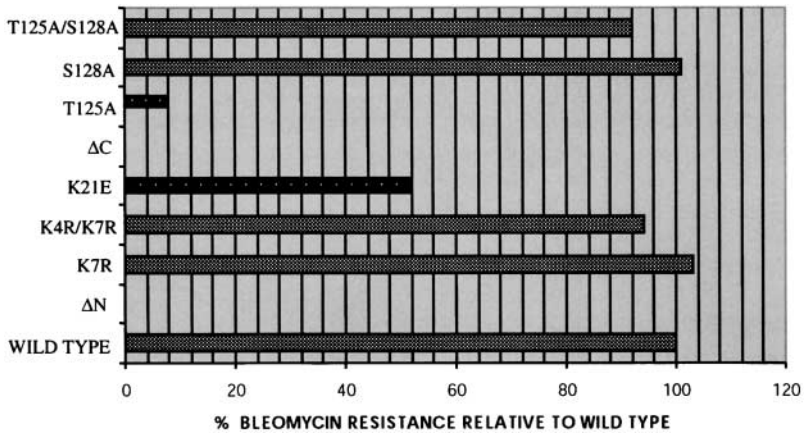

FIGURE 7.—*hta1tpe* alleles are hypersensitive to DSB production. Ura3⁻ cells carrying *hta1tpe* alleles were grown on SC + FOA in the presence of 15 mU/ml bleomycin. The percentage of viable cells in an *hta1tpe* allele was normalized to wild-type cells treated with the same level of bleomycin on SC + FOA plates. This value, described in MATERIALS AND METHODS, represents the decrease in bleomycin resistance at 15 mU/ml in a specific allele relative to wild-type cells and allows a direct comparison between viability and silencing on SC + FOA plates. Ura⁻ strains produce a lower number of colonies on FOA media relative to growth on SC, thereby allowing for a direct comparison between silencing and bleomycin sensitivity. Growth on SC produced a qualitatively similar result. FY406 cells carried a plasmid-borne copy of wild-type *HTA1*, *hta1ΔN*, *hta1K7R*, *hta1K4R/K7R*, *hta1K21E-2*, *hta1ΔC*, *hta1T125A*, *hta1S128A*, and *hta1T125A/S128A*. Gray stippled bars refer to values not statistically different from those of wild type; black stippled bars refer to values significantly lower than those of wild-type resistance. Δ*N*, *K21-2*, and *T125A* also had slow growth rates associated with the loss of silencing. Values for Δ*N* and Δ*C* (not visible in chart) are 0.112 and 0.031%, respectively.

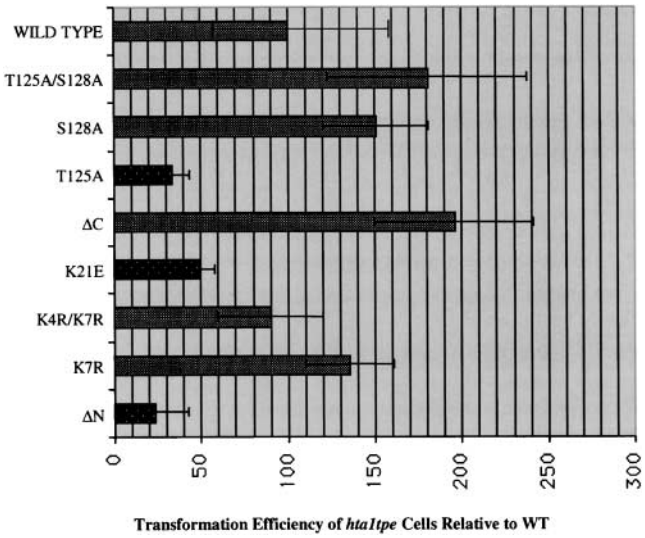

FIGURE 8.—Plasmid repair defects of *hta1tpe* alleles. *Sac*I-digested pRS316 DNA was transformed into FY406 cells containing plasmid-encoded wild-type *HTA1* ($n = 23$), *hta1*Δ*N* ($n = 5$), *hta1K7R* ($n = 6$), *hta1K4R/K7R* ($n = 5$), *hta1K21E* ($n = 5$), *hta1*Δ*C* ($n = 14$), *hta1T125A* ($n = 7$), *hta1S128A* ($n = 6$), or *hta1T125A/S128A* ($n = 5$). *n* refers to the number of trials. The number of transformants for each allele was normalized to the internal wild-type control in each trial. The data are presented as the mean of all trials for each allele ± 95% confidence limits. Gray stippled bars indicate values not statistically different from wild type at $P = 0.05$; black stippled bars refer to alleles that displayed a significantly lower level of plasmid end joining.

cells. These data are consistent with the predominant use of homologous recombination in the repair of DSBs at doses of bleomycin below 20 mU/ml (data not shown; MARTIN *et al.* 1999). In *hta1*Δ*N* cells, however, viability decreased 2-fold in the *yku70* null allele compared to *YKU70* cells at 15 mU/ml bleomycin, indicating the higher use of the yKu system of DSB repair in these cells ($P < 0.005$; Figure 9A). A more dramatic effect was observed in the *hta1T125A* allele. These cells displayed a 3.5-fold and 120-fold increase in the dependency of DSB repair on yKu at 5 mU/ml and 15 mU/ml of bleomycin, respectively. Hence, the data are consistent with the proposed relationship between yKu dependence in wild-type and *hta1tpe* alleles.

The second prediction of this hypothesis is an altered equilibrium between telomeric yKu and DSB-bound yKu in the *hta1tpe* alleles. We therefore tested the dependence of silencing on yKu in wild-type and *hta1tpe* cells in the presence or absence of bleomycin. This assay is limited by the substantial decrease in silencing in *yku70* cells (220-fold in our strains; PORTER *et al.* 1996; EVANS *et al.* 1998). However, both Δ*N* and *T125A* alleles displayed a further >7-fold and >2.5-fold decrease in silencing, respectively, in the absence of yKu ($P < 0.01$; Figure 9B). In summary, these data suggest that histone H2A contributes to the maintenance of yKu-dependent silencing even in the absence of DNA damage.

DISCUSSION

In this study, we demonstrate a role for the amino and carboxyl tails of histone H2A in telomeric silencing, a property not shared by histone H2B (THOMPSON *et al.* 1994). This represents the first evidence for the participation of histone H2A in TPE. Most of these *hta1tpe* alleles share a common set of phenotypes in several cellular processes (Table 2). First, all *hta1tpe* alleles suppress the *lys2-128*δ mutation. This Spt$^-$ phenotype is likely to be mediated through alterations in chromatin structure. The *T125A* allele confers a 2000-fold increase in the Spt$^-$ phenotype relative to wild-type cells. In contrast, the *T125AS128A* allele conferred only a 7-fold increase relative to wild-type cells, although the *S128A* allele alone generated a wild-type phenotype. These data suggest that the mutant *S128A* has a strong influence on the *T125A* phenotype and therefore clearly participates in this process.

Second, the *hta1tpe* alleles Δ*N*, *S21E-2*, and *T125A* confer a decrease in TPE in the presence of bleomycin relative to the 0-mU/ml bleomycin values. In addition, hypersensitivity to bleomycin is observed in most *hta1tpe* alleles (Δ*N*, *S21E-2*, *T125A*, Δ*C*). Indeed, the two *hta1tpe* alleles tested (Δ*N*, *T125A*) are more sensitive to bleomycin in the absence of yKu70. Third, all of the *hta1tpe* alleles that conferred bleomycin-induced loss of silencing also displayed a decrease in the efficiency of NHEJ in a cohesive-end plasmid-joining assay. Taken together with the minimal effects of γ-irradiation, these data implicate a defect in yKu-mediated repair events—a major pathway for repair of bleomycin-induced DSBs and plasmid rejoining (MAGES *et al.* 1996; MILNE *et al.* 1996; MARTIN *et al.* 1999; MILLS *et al.* 1999; MOORE *et al.* 2000). Fourth, the link between silencing, yKu, and histone H2A is further strengthened by the observation that TPE Δ*N* and *T125A* is additionally compromised in the absence of yKu. These studies indicate that the amino- and carboxyl-terminal tails of H2A are essential for wild-type levels of yKu-dependent TPE and DSB repair.

These phenotypes are not likely to be the consequence of nonspecific or global effects of *hta1tpe* alleles. First, as noted in the RESULTS, growth rate, H2A abundance, and telomere size are not significantly altered in the *hta1tpe* alleles (Table 1). Second, changes in *URA3* transcription are unlikely to be the consequence of a loss of H2A-mediated repression of the basal transcription of some genes (LENFANT *et al.* 1996). This latter process is dependent on the Hir proteins and on components of the SWI/SNF complex (DIMOVA *et al.* 1999; RECHT and OSLEY 1999). In contrast, the pathway of *URA3* transcriptional regulation involves a specific Ppt1 activator system and there is no evidence for the involvement of SWI/SNF in *URA3* transcription (ROY *et al.* 1990). Third, some *hta1* alleles within the amino terminus are defective in the SWI/SNF-mediated chromatin remodeling (HIRSCHHORN *et al.* 1995). Of the four amino-

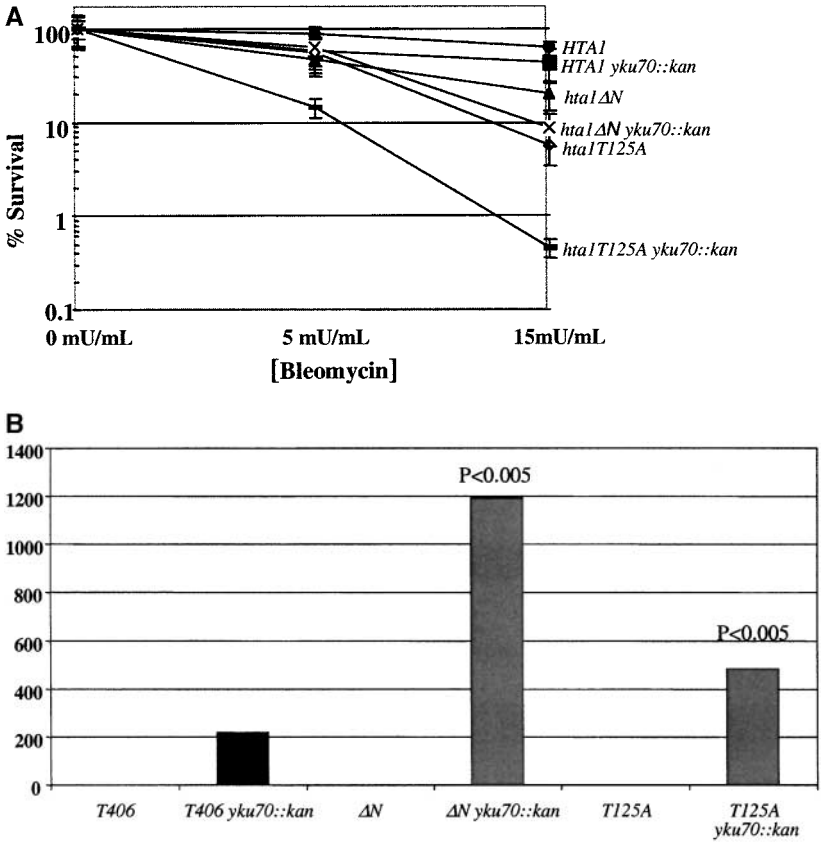

FIGURE 9.—The influence of yKu70 on *hta1tpe* silencing and bleomycin sensitivity. (A) Sensitivity of *hta1ΔN* and *hta1T125A* to bleomycin in the presence or absence of yKu70. Cells from each allele were plated at varying dilutions on SC and SC + bleomycin plates at the indicated concentrations. The results are presented on a semilog scale. In each case, the 95% confidence limits are indicated. Strain designations are shown on the right. Note that these values differ from those in Figure 7 since cells were grown on SC plates lacking FOA, which displays a lower sensitivity to bleomycin. (B) Sensitivity of TPE in wild-type and *hta1tpe* alleles that lack yKu. Each strain indicated was plated onto SC + FOA at 10-fold dilutions and the cells counted at the appropriate dilution. The ratio (FOA^r/SC) was determined and used to correct for the lowered viability on FOA as described in A and in MATERIALS AND METHODS. Each *YKU70* strain was set to a value of 1 and the fold decrease in FOA resistance in *yku70* strains was plotted on the semilog plot. *HTA1*, *hta1ΔN*, and *hta1T125A* alleles had a significantly greater loss in silencing than the corresponding allele had in the absence of Yku70.

terminal alleles investigated in that study (*ΔN*, *S19F*, *S19P*, *S21E*), the order of alleles that conferred *swi/snf* phenotypes is $S19F \gg S19P = \Delta N > S21E$. In contrast, neither *S19F* nor *S19P* displayed a loss of telomeric silencing (data not shown). Thus, there is no correlation between the *hta1* alleles involved in *SWI/SNF* gene activation and the *hta1tpe* alleles. Fourth, the enhanced sensitivity to bleomycin in *hta1tpe* alleles is not due to random fragmentation since γ-irradiation has no effect on viability relative to wild type (data not shown).

Both histones H2A1 and H2A3 function in telomeric silencing: Mutations in *HTA3*, which encodes the yeast H2A.Z variant, cannot complement *hta1* mutations, suggesting that H2A1 and H2A3, at least in part, perform unique functions (JACKSON and GOROVSKY 2000; SANTISTEBAN *et al.* 2000; REDON *et al.* 2002). Deletion of *HTA3* results in a partial loss of *HMR* silencing and a significant (~25-fold) decrease in FOA^r colonies at the *URA3*-marked VII_L telomere (DHILLON and KAMAKAKA 2000). Interestingly, this magnitude of silencing loss is similar to the defects observed in the *ΔN* allele of *H2A1*. It is likely therefore that both H2A1 and H2A3 function in the formation or stability of telomeric heterochromatin, although the functional relationship between these variants remains unknown.

Internal regulatory circuits governing H2A function: A comparison of phenotypes defines several distinct classes of *hta1tpe* mutants. The first class consists of mutations that are defective in silencing, the Spt^+ phenotype, and the DNA damage response. These include *ΔN*, *K21E*, and *T125A*. One allele, *ΔC*, defines a second class, which is not defective in plasmid rejoining, but is responsive to bleomycin. This allele follows a pathway distinct from the *T125A/S128A* interaction within the C-terminal tail microenvironment. Finally, the *K7R* and *K4R/K7R* alleles define a third class that display defects only in telomeric silencing and in the Spt^+ phenotype, but not in DNA damage response. These mutations act within the microenvironment of the amino-terminal tail and may define a unique pathway of H2A in TPE and Spt^+ phenotypes unrelated to DNA damage. Therefore, it is likely that loss of the amino terminus confers defects through either structural modification(s) of histone H2A or loss of as-yet-unidentified binding sites for silencing-related proteins.

One interesting feature of our results is the presence of unique combinatorial phenotypes within a specific microenvironment. Three such cases were uncovered in these studies. First, in the amino-terminal tail, K4R alone confers a wild-type level of silencing. In contrast, K7R hyper-repressed telomeric silencing while the K4R/K7R double mutant conferred a significant disruption of TPE. Hence, the presence of K4R antagonizes the positive effect of K7R, suggesting a negative interference between the two residues. Curiously, when both residues are changed to a neutral residue, the K7R elevated levels

were again reached. Differential acetylation and deacetylation or charge interference of these residues may therefore serve as a regulatory switch to promote or to diminish telomeric silencing.

Second, we found that the defects of *T125A* are not observed in either the *S128A* or the *T125A/S128A* double-mutant cells both of which display wild-type phenotypes. These data suggest a common regulatory circuit between T125 and S128. Since the *S128A* phenotype is always dominant in double mutants, we propose that T125 acts to inhibit an S128 positive signal for TPE.

The involvement of amino acid modifications in multiple H2A functions: Our data suggest that both amino- and carboxyl-terminal tails of H2A perform functions important for telomeric silencing and that these functions are likely to be mediated, in part, through post-translational modifications. Within the amino-terminal tail, K4 has been shown to be a target for the yeast NuA4 acetylase catalytic subunit, Esa1p, *in vitro.* Similarly, K7 is a target of acetylation and deacetylation *in vivo* and *in vitro* (Clarke *et al.* 1999; Ohba *et al.* 1999; Suka *et al.* 2001; Goll and Bestor 2002). Indeed, K7 is deacetylated within heterochromatic regions *in vivo* (Suka *et al.* 2001), possibly by the K7-specific Hos3 deacetylase (Carmen *et al.* 1999). Surprisingly, our data suggest that acetylation, rather than deacetylation, of K4 may be required for efficient silencing, unlike the acetylation/deacetylation pattern within the aminotermini of histones H3 and H4 (Grunstein 1997). A comprehensive study of histone acetylation in the amino terminus in repressed and derepressed states will be required to resolve these issue. Although methylation of histone H2A lysines is a formal possibility, to date no description of histone methylases has been targeted to either H2A or H2B.

In contrast, the pattern of the *K21* mutation suggests that a positive or neutral charge is important to maintain silencing, most likely through a charge requirement for the local structure of histone H2A. Hence, the amino terminus of H2A may participate in a mechanistically unique facilitation of telomeric silencing. Two classes of *K21E* phenotypes were found after treatment of different *K21E* colonies with bleomycin: one highly sensitive to bleomycin and the other sensitive to wild-type values, a possible consequence of an epigenetic switch between histone H2A states or copy-number variation within the population.

Deletion of the C-terminal tail (Δ120–131) results in a loss of the vast majority of H2A phosphorylation, suggesting that the C terminus contains the major site(s) of phosphorylation under steady-state growth. Previous studies have demonstrated that S128 is hyperphosphorylated in response to several forms of DNA damage agents (Downs *et al.* 2000; Bassing *et al.* 2002). This hyperphosphorylation in yeast and in other species plays a definitive role in DSB repair. In striking contrast, within the context of the C terminus, the functional interaction between T125 and S128 is critical for all of the phenotypes tested in our study. A role for phosphorylation of T125 is supported by the lack of a silencing defect in *T125E* mutants. Cells blocked in the phosphorylation of T125 and/or S128 still display a significant level of H2A phosphorylation, presumably arising from the phosphorylation of S121.

Conversely, elimination of S121 phosphorylation results in the hyperphosphorylation of T125 and/or S128. These data suggest that a regulatory circuit ensures site-independent phosphorylation within the carboxyl terminus. We cannot rule out the formal possibility that the amino terminus or globular domain is hyperphosphorylated in response to mutations in carboxyl-terminal phosphorylation sites.

However, the finding that the inhibition of growth rate is far more severe in *S121A/ T125A/S128A* triple mutants than in cells containing a deletion of the carboxyl terminus or the *S128A/T125A* double mutant is consistent with the functional redundancy of these three sites. Functional redundancy within H2A histone C-terminal regions is also suggested by the presence of multiple phosphoserine residues within the C-terminal tail of the major Tetrahymena H2A variants (Fusauchi and Iwai 1984). Since the antibody against a phosphorylated C-terminal peptide in a previous study could not detect phosphorylation in the absence of DNA damage (Downs *et al.* 2000), our studies provide the first insights into yeast H2A phosphorylation under non-DNA damage conditions.

The flexible requirement for carboxyl-terminal phosphorylation events may also be related to alternative functions that alter the stability of specific chromatin domains (*e.g.*, telomeric and Spt^+ chromatin). These data raise the possibility that promiscuous phosphorylation under steady-state conditions may be related to interdependent T125/S128 functional interactions.

H2A involvement in telomeric silencing and alternative Spt^+ effects on gene expression: A common chromatin structure? The amino-terminal tails of H2A1 (encoded by *SPT11*) and H2B1 (encoded by *SPT12*) form domains that are required for the Spt^+ phenotype. This phenotype is mediated in part through Spt4 and Spt5 and specific N-terminal domains in histone H2A (Recht *et al.* 1996). Spt4 and Spt5 complexes have a critical role in transcriptional elongation, which is likely to be important in breaking nucleosomal barriers (Recht *et al.* 1996; Hartzog *et al.* 1998; Yamaguchi *et al.* 2001). However, the binding of Spt4 and Spt5 remains to be critically tested. In contrast, Spt6 associates preferentially with histones H3 and H4 (Bortvin and Winston 1996; Yamaguchi *et al.* 2001). Spt6 associates with histone H3 through an ATP-independent chromatin assembly activity (Bortvin and Winston 1996), strongly suggesting that its primary role is in the remodeling of chromatin. Histone H2A-mediated transcriptional repression appears to be mediated through a

HIR-dependent targeting of genes to specific chromatin regions. (Recht *et al.* 1996).

This study has revealed a functional linkage between the chromatin formed in telomeric silencing and the Spt^+ repression. All of the *hta1tpe* alleles also have Spt^- phenotypes, suggesting that both the amino and carboxyl termini of H2A share elements that influence chromatin states in both chromosomal regions. Among these, we identified specific *hta1tpe* alleles that confer profound effects on *lys2-128*δ suppression. A total of 10–50% of *K4R/K7R*, *K21E*, and *T125A* cells are Lys^+, similar to the values observed in strong *spt* mutants such as *spt5* (Swanson *et al.* 1991). In contrast, Δ*N* and Δ*C* have less severe Spt^- phenotypes than single missense mutations have within the tail regions, indicating differences in alterations of a microenvironment from loss of the entire domain. Hence, both histone structure and site-specific modifications in H2A tails may contribute to chromatin remodeling.

The notion of functionally overlapping roles for histone H2A in TPE and Spt^+ phenotypes is supported by other studies. First, Spt^- phenotypes are conferred by *hir1* and *hir2* mutations (Sherwood *et al.* 1993) and Hir proteins are involved in an alternative pathway for TPE (Sherwood and Osley 1991; Sharp *et al.* 2001; Krawitz *et al.* 2002). Second, the potential H2A1 binding protein, Spt16 (Ho *et al.* 2002), physically associates with Pob3 and the Sas3 acetylase to form the NuA3 acetylation complex, which is involved in activation, repression, and silencing activities (Wittmeyer *et al.* 1999; John *et al.* 2000; Formosa *et al.* 2001). Third, the histone H2A-interacting protein Act3/Arp4 is a component of the NuA4 histone acetylation complex that acetylates H2A at both K4 and K7 *in vitro* (Ohba *et al.* 1999; Galarneau *et al.* 2000; Vogelauer *et al.* 2000). One of the major challenges for the future is to determine the contributions of specific residues within histone H2A termini to associations with a common or overlapping set of regulatory factors through an as-yet-undeciphered H2A "histone code" (Jenuwein and Allis 2001).

The dual role of H2A in DNA damage and TPE: Several results suggest a relationship between H2A in telomeric silencing and DSB repair. These include (a) a loss in silencing rates in a subset of *hta1tpe* alleles (Δ*N*, *K21E*, Δ*C*, *T125A*) after treatment with low doses of bleomycin, (b) hypersensitivity to higher doses of bleomycin (Δ*N*, *K21E*, *T125A*), and (c) a reduction in nonhomologous end joining of digested plasmids (Δ*N*, *K21E*, *T125A*).

Our data indicate that *hta1tpe* and wild-type cells exhibit similar sensitivities to UV- and γ-irradiation (data not shown). Furthermore, silencing of only one allele (*K21E*) was decreased fourfold following γ-treatment (data not shown). As noted, bleomycin-induced DSBs and plasmid DSBs are repaired at low doses by homologous recombination while higher doses are highly sensitive to the absence of yKu (Mages *et al.* 1996; Milne *et al.* 1996; Martin *et al.* 1999; Mills *et al.* 1999). These data suggest the involvement of yKu-dependent repair pathways in silencing after DNA damage in *hta1tpe* alleles. Indeed, our current studies demonstrate a direct role of yKu in resistance to bleomycin at low doses of bleomycin. The role of S128 phosphorylated H2A induced by DNA damage remains uncertain. Although yeast *hta1* and *hta2* mutations in S128 (or in the required Mec1p SQ motif) increase methyl methanesulfonate and/or phleomycin sensitivity, the pathway of DNA repair affected by these mutations appears to be independent of both yKu and Rad52 (Downs *et al.* 2000).

Previous studies suggested that DSB formation leads to a Rad53-dependent checkpoint arrest in G2. This arrest induces a migration of yKu and Sir3 from the telomeres (and subtelomeric regions) to the DSB sites where yKu assembles the DNA NHEJ repair machinery (Martin *et al.* 1999; McAinsh *et al.* 1999; Mills *et al.* 1999). The subsequent depletion of shared silencing and DNA damage repair factors, such as yKu, are likely to explain the decrease in telomeric silencing.

We propose that the *hta1tpe* alleles act in an analogous fashion after bleomycin-induced G2 arrest that requires the yKu heterodimer for efficient repair. In this model, one function for H2A at the telomere is to provide a "lock" against the promiscuous loss of silencing/DNA repair factors from the telomere, even in the absence of DNA damage. The phenotypes of some *hta1* alleles may therefore be due to a failure to form the appropriate yKu-dependent heterochromatic structure. In support of this, we have shown that both *hta1tpe* alleles tested contributed an additional loss of silencing in the absence of yKu, indicating the direct involvement of histone H2A in yKu-dependent telomeric silencing.

How then are the silencing defects of these alleles reconciled with their hypersensitivity to bleomycin? Clearly, an increased pool of silencing factors is unlikely to cause a disruption of DNA repair. One possible explanation is that the heterochromatin structures required for TPE and DSB repair are similar. In this model, *hta1tpe* alleles would be functionally defective at both sites.

We favor a more parsimonious explanation in which bleomycin-induced loss of silencing, DNA repair, and viability are related to H2A defects at the telomere (Figure 10). We propose that the *hta1tpe* alleles alter the structure of telomeric/subtelomeric domains, leading to a decreased retention of silencing/repair factors, even under non-DNA damage conditions. At low concentrations of bleomycin, sufficient DNA damage would be produced in *hta1tpe* alleles that may provoke a stronger signal for the yKu-dependent DSB repair pathway and, consequently, an enhanced loss of silencing/repair factors to DSBs. The *hta1tpe* allele phenotypes cannot be explained as a secondary consequence of randomly fragmented genomic DNA, given that *hta1tpe* alleles have wild-type sensitivities to γ-irradiation. In ad-

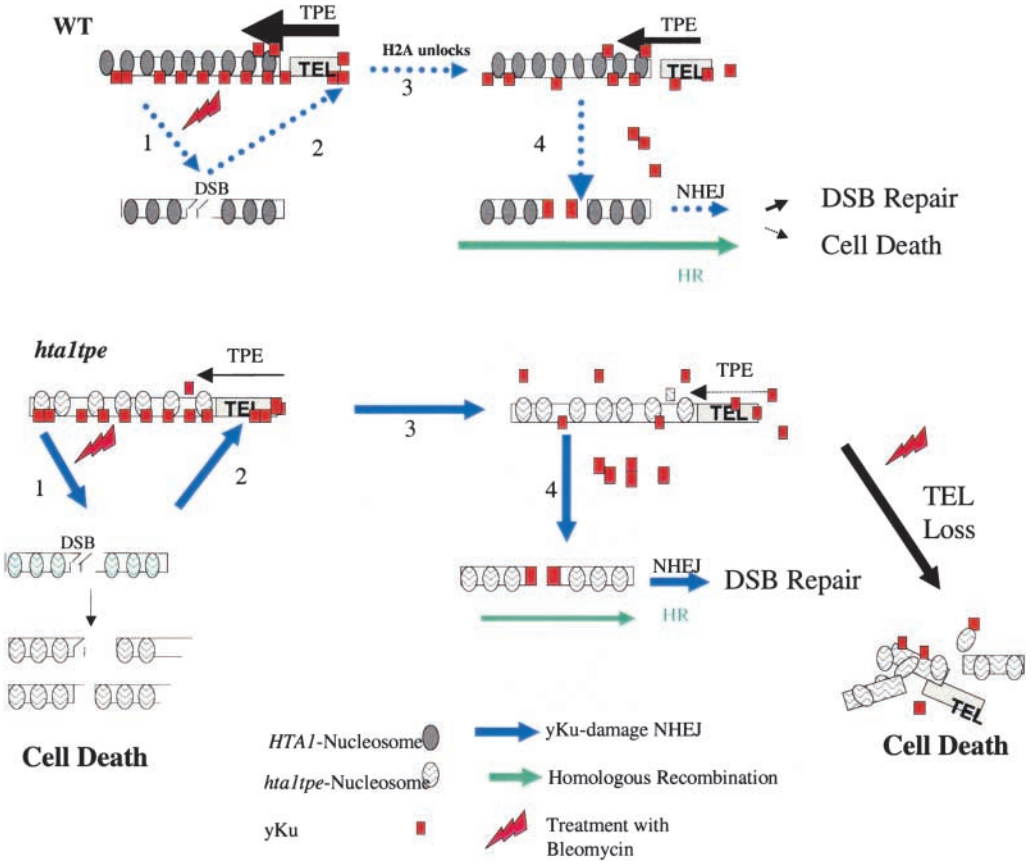

FIGURE 10.—A model relating H2A function in TPE and DSB repair. (WT) In the absence of DNA damage, histone H2A promotes the retention of telomeric yKu70 and other silencing/repair factors leading to efficient TPE. In the presence of 5–20 mU/ml bleomycin used in these studies, a slight dose-dependent decrease in viability is observed, most likely reflecting a corresponding increase in DSBs. DSB repair is likely to proceed through both homologous recombination (HR) and yKu-mediated NHEJ at these levels of bleomycin. Since wild-type cells are highly refractory to DSBs at these doses, only a low level induction of the Rad53 pathway is likely, leading to a minor loss of yKu and a slightly lowered TPE efficiency. Step 1, formation of DSB; step 2, induction of Rad53 pathway; step 3, loss of H2A lock; step 4, release of yKu from telomere to the DSB, resulting in NHEJ. The intensity of the lines corresponds to the relative pathway efficiencies at the doses tested. (*hta1tpe*) The *hta1tpe* mutations result in a more open chromatin state that confers further decreases in TPE in the absence of the yKu heterodimer. Following treatment with bleomycin, defects in the H2A lock would facilitate the response of the Rad53 pathway, resulting in an increase in yKu-dependent NHEJ and a loss in telomeric silencing. The decreased viability in *hta1tpe* mutants is proposed to be the consequence of direct alterations in telomeric structure resulting in terminal deletions. However, the less likely possibility of genomic fragmentation is shown by the dotted lines. The pathway is as described above.

dition, bleomycin has specificity for more open chromatin-domain nucleosomal regions (MOORE 1989). Hence, any overall DNA damage defect is confined to bleomycin-induced DSBs, lessening, but not excluding, the likelihood of lethality due to gross chromosomal fragmentation. Given the open conformation of subtelomeric regions after loss of silencing, we speculate that lethality may be due in large part to terminal truncation.

In summary, our data suggest a relationship between TPE, Spt^+ chromatin reorganization, nonhomologous end joining, and H2A function. We propose that H2A acts as a telomeric tether to prevent promiscuous mobilization of heterochromatic factors. The examination of chromatin structure at both telomeres and DSBs in these alleles, and the identification of factors that interact with H2A, will ultimately help in understanding the mechanistic basis of histone H2A function in the remodeling of telomeric heterochromatin.

We thank Fred Winston for providing strains and Mary Ann Osley for the kind gift of strains before publication. We also thank Carol W. Moore, Mary Ann Osley, James Haber, Thomas D. Petes, Gilbert Morris, Linda Hyman, and E. B. Hoffman for stimulating discussions. We acknowledge the technical support of Mark Tidwell and the advice and assistance of former and present members of our laboratory. This study was funded by National Science Foundation grant MCB-0084460 and National Institutes of Health grant GM-56526 (to A.J.L.), an LEQSF grant 97-00-RD-A-130 (to G.R.G.), a Dissertation Year Scholarship (to H.R.W.), and the Tulane Cancer Center (to H.L.).

LITERATURE CITED

BASSING, C. H., K. F. CHUA, J. SEKIGUCHI, H. SUH, S. R. WHITLOW *et al.*, 2002 Increased ionizing radiation sensitivity and genomic instability in the absence of histone H2AX. Proc. Natl. Acad. Sci. USA **99:** 8173–8178.

BAUR, J. A., Y. ZOU, J. W. SHAY and W. E. WRIGHT, 2001 Telomere position effect in human cells. Science **292:** 2075–2077.

BORTVIN, A., and F. WINSTON, 1996 Evidence that Spt6p controls chromatin structure by a direct interaction with histones. Science **272:** 1473–1476.

BOULTON, S. J., and S. P. JACKSON, 1998 Components of the Ku-dependent non-homologous end-joining pathway are involved in telomeric length maintenance and telomeric silencing. EMBO J. **17:** 1819–1828.

BRIGGS, S. D., M. BRYK, B. D. STRAHL, W. L. CHEUNG, J. K. DAVIE *et al.*, 2001 Histone H3 lysine 4 methylation is mediated by Set1 and required for cell growth and rDNA silencing in Saccharomyces cerevisiae. Genes Dev. **15:** 3286–3295.

CARMEN, A. A., P. R. GRIFFIN, J. R. CALAYCAY, S. E. RUNDLETT, Y. SUKA *et al.*, 1999 Yeast HOS3 forms a novel trichostatin A-insensitive

homodimer with intrinsic histone deacetylase activity. Proc. Natl. Acad. Sci. USA **96:** 12356–12361.

Carmen, A. A., L. Milne and M. Grunstein, 2002 Acetylation of the yeast histone H4 N terminus regulates its binding to heterochromatin protein SIR3. J. Biol. Chem. **277:** 4778–4781.

Clark-Adams, C. D., and F. Winston, 1987 The SPT6 gene is essential for growth and is required for delta-mediated transcription in Saccharomyces cerevisiae. Mol. Cell. Biol. **7:** 679–686.

Clark-Adams, C. D., D. Norris, M. A. Osley, J. S. Fassler and F. Winston, 1988 Changes in histone gene dosage alter transcription in yeast. Genes Dev. **2:** 150–159.

Clarke, A. S., J. E. Lowell, S. J. Jacobson and L. Pillus, 1999 Esa1p is an essential histone acetyltransferase required for cell cycle progression. Mol. Cell. Biol. **19:** 2515–2526.

Cockell, M., M. Gotta, F. Palladino, S. G. Martin and S. M. Gasser, 1998a Targeting Sir proteins to sites of action: a general mechanism for regulated repression. Cold Spring Harbor Symp. Quant. Biol. **63:** 401–412.

Cockell, M., H. Renauld, P. Watt and S. M. Gasser, 1998b Sif2p interacts with Sir4p amino-terminal domain and antagonizes telomeric silencing in yeast. Curr. Biol. **8:** 787–790.

de Bruin, D., S. M. Kantrow, R. A. Liberatore and V. A. Zakian, 2000 Telomere folding is required for the stable maintenance of telomere position effects in yeast. Mol. Cell. Biol. **20:** 7991–8000.

de Bruin, D., Z. Zaman, R. A. Liberatore and M. Ptashne, 2001 Telomere looping permits gene activation by a downstream UAS in yeast. Nature **409:** 109–113.

Dhillon, N., and R. T. Kamakaka, 2000 A histone variant, Htz1p, and a Sir1p-like protein, Esc2p, mediate silencing at HMR. Mol. Cell **6:** 769–780.

Dimova, D., Z. Nackerdien, S. Furgeson, S. Eguchi and M. A. Osley, 1999 A role for transcriptional repressors in targeting the yeast Swi/Snf complex. Mol. Cell **4:** 75–83.

Downs, J. A., N. F. Lowndes and S. P. Jackson, 2000 A role for Saccharomyces cerevisiae histone H2A in DNA repair. Nature **408:** 1001–1004.

Enomoto, S., and J. Berman, 1998 Chromatin assembly factor I contributes to the maintenance, but not the re-establishment, of silencing at the yeast silent mating loci. Genes Dev. **12:** 219–232.

Evans, S. K., M. L. Sistrunk, C. I. Nugent and V. Lundblad, 1998 Telomerase, Ku, and telomeric silencing in Saccharomyces cerevisiae. Chromosoma **107:** 352–358.

Formosa, T., P. Eriksson, J. Wittmeyer, J. Ginn, Y. Yu *et al.*, 2001 Spt16-Pob3 and the HMG protein Nhp6 combine to form the nucleosome-binding factor SPN. EMBO J. **20:** 3506–3517.

Fusauchi, Y., and K. Iwai, 1984 Tetrahymena histone H2A. Acetylation in the N-terminal sequence and phosphorylation in the C-terminal sequence. J. Biochem. **95:** 147–154.

Galarneau, L., A. Nourani, A. A. Boudreault, Y. Zhang, L. Heliot *et al.*, 2000 Multiple links between the NuA4 histone acetyltransferase complex and epigenetic control of transcription. Mol. Cell **5:** 927–937.

Gasser, S. M., and M. M. Cockell, 2001 The molecular biology of the SIR proteins. Gene **279:** 1–16.

Goll, M. G., and T. H. Bestor, 2002 Histone modification and replacement in chromatin activation. Genes Dev. **16:** 1739–1742.

Gottschling, D. E., 1992 Telomere-proximal DNA in *Saccharomyces cerevisiae* is refractory to methyltransferase activity in vivo. Proc. Natl. Acad. Sci. USA **89:** 4062–4065.

Gottschling, D. E., O. M. Aparicio, B. L. Billington and V. A. Zakian, 1990 Position effect at S. cerevisiae telomeres: reversible repression of Pol II transcription. Cell **63:** 751–762.

Green, G. R., 2001 Phosphorylation of histone variant regions in chromatin: Unlocking the linker? Biochem. Cell Biol. **79:** 275–287.

Green, G. R., and D. L. Poccia, 1989 Phosphorylation of sea urchin histone CS H2A. Dev. Biol. **134:** 413–419.

Green, G. R., L. C. Gustavsen and D. L. Poccia , 1990 Phosphorylation of plant H2A histones. Plant Physiol. **93:** 1241–1245.

Grunstein, M., 1997 Molecular model for telomeric heterochromatin in yeast. Curr. Opin. Cell Biol. **9:** 383–387.

Grunstein, M., 1998 Yeast heterochromatin: regulation of its assembly and inheritance by histones. Cell **93:** 325–328.

Hartzog, G. A., T. Wada, H. Handa and F. Winston, 1998 Evidence that Spt4, Spt5, and Spt6 control transcription elongation by RNA polymerase II in Saccharomyces cerevisiae. Genes Dev. **12:** 357–369.

Hecht, A., T. Laroche, S. Strahl-Bolsinger, S. M. Gasser and M. Grunstein, 1995 Histone H3 and H4 N-termini interact with SIR3 and SIR4 proteins: a molecular model for the formation of heterochromatin in yeast. Cell **80:** 583–592.

Hirschhorn, J. N., A. L. Bortvin, S. L. Ricupero-Hovasse and F. Winston, 1995 A new class of histone H2A mutations in Saccharomyces cerevisiae causes specific transcriptional defects in vivo. Mol. Cell. Biol. **15:** 1999–2009.

Ho, A., A. Gruhler, A. Heilbut, G. D. Bader, L. Moore *et al.*, 2002 Systematic identification of protein complexes in Saccharomyces cerevisiae by mass spectrometry. Nature **415:** 180–183.

Hoppe, G. J., J. C. Tanny, A. D. Rudner, S. A. Gerber, S. Danaie *et al.*, 2002 Steps in assembly of silent chromatin in yeast: Sir3-independent binding of a Sir2/Sir4 complex to silencers and role for Sir2-dependent deacetylation. Mol. Cell. Biol. **22:** 4167–4180.

Imai, S., C. M. Armstrong, M. Kaeberlein and L. Guarente, 2000 Transcriptional silencing and longevity protein Sir2 is an NAD-dependent histone deacetylase. Nature **403:** 795–800.

Jackson, J. D., and M. A. Gorovsky, 2000 Histone H2A.Z has a conserved function that is distinct from that of the major H2A sequence variants. Nucleic Acids Res. **28:** 3811–3816.

Jenuwein, T., and C. D. Allis, 2001 Translating the histone code. Science **293:** 1074–1080.

John, S., L. Howe, S. T. Tafrov, P. A. Grant, R. Sternglanz *et al.*, 2000 The something about silencing protein, Sas3, is the catalytic subunit of NuA3, a yTAF(II)30-containing HAT complex that interacts with the Spt16 subunit of the yeast CP (Cdc68/Pob3)-FACT complex. Genes Dev. **14:** 1196–1208.

Kahana, A., and D. E. Gottschling, 1999 DOT4 links silencing and cell growth in Saccharomyces cerevisiae. Mol. Cell. Biol. **19:** 6608–6620.

Krawitz, D. C., T. Kama and P. D. Kaufman, 2002 Chromatin assembly factor I mutants defective for PCNA binding require Asf1/Hir proteins for silencing. Mol. Cell. Biol. **22:** 614–625.

Krogan, N. J., J. Dover, S. Khorrami, J. F. Greenblatt, J. Schneider *et al.*, 2002 COMPASS, a histone H3 (lysine 4) methyltransferase required for telomeric silencing of gene expression. J. Biol. Chem. **277:** 10753–10755.

Kyrion, G., K. Liu, C. Liu and A. J. Lustig, 1993 RAP1 and telomere structure regulate telomere position effects in *Saccharomyces cerevisiae*. Genes Dev. **7:** 1146–1159.

Lachner, M., D. O'Carroll, S. Rea, K. Mechtler and T. Jenuwein, 2001 Methylation of histone H3 lysine 9 creates a binding site for HP1 proteins. Nature **410:** 116–120.

Landry, J., A. Sutton, S. T. Tafrov, R. C. Heller, J. Stebbins *et al.*, 2000 The silencing protein SIR2 and its homologs are NAD-dependent protein deacetylases. Proc. Natl. Acad. Sci. USA **97:** 5807–5811.

Laroche, T., S. G. Martin, M. Gotta, H. C. Gorham, F. E. Pryde *et al.*, 1998 Mutation of yeast Ku genes disrupts the subnuclear organization of telomeres. Curr. Biol. **8:** 653–656.

Lenfant, F., R. K. Mann, B. Thomsen, X. Ling and M. Grunstein, 1996 All four core histone N-termini contain sequences required for the repression of basal transcription in yeast. EMBO J. **15:** 3974–3985.

Liu, C., X. Mao and A. J. Lustig, 1994 Mutational analysis defines a C-terminal tail domain of RAP1 essential for telomeric silencing in *Saccharomyces cerevisiae*. Genetics **138:** 1025–1040.

Luger, K., and T. J. Richmond, 1998 The histone tails of the nucleosome. Curr. Opin. Genet. Dev. **8:** 140–146.

Luger, K., A. W. Mader, R. K. Richmond, D. F. Sargent and T. J. Richmond, 1997 Crystal structure of the nucleosome core particle at 2.8 A resolution. Nature **389:** 251–260.

Luo, K., M. A. Vega-Palas and M. Grunstein, 2002 Rap1-Sir4 binding independent of other Sir, yKu, or histone interactions initiates the assembly of telomeric heterochromatin in yeast. Genes Dev. **16:** 1528–1539.

Lustig, A. J., 1998 Mechanisms of silencing in Saccharomyces cerevisiae. Curr. Opin. Genet. Dev. **8:** 233–239.

Mages, G. J., H. M. Feldmann and E. L. Winnacker, 1996 Involvement of the Saccharomyces cerevisiae HDF1 gene in DNA double-strand break repair and recombination. J. Biol. Chem. **271:** 7910–7915.

Martin, S. G., T. Laroche, N. Suka, M. Grunstein and S. M. Gasser,

1999 Relocalization of telomeric Ku and SIR proteins in response to DNA strand breaks in yeast. Cell **97:** 621–633.

McAinsh, A. D., S. Scott-Drew, J. A. Murray and S. P. Jackson, 1999 DNA damage triggers disruption of telomeric silencing and Mec1p-dependent relocation of Sir3p. Curr. Biol. **9:** 963–966.

Mills, K. D., D. A. Sinclair and L. Guarente, 1999 MEC1-dependent redistribution of the Sir3 silencing protein from telomeres to DNA double-strand breaks. Cell **97:** 609–620.

Milne, G. T., S. Jin, K. B. Shannon and D. T. Weaver, 1996 Mutations in two Ku homologs define a DNA end-joining repair pathway in Saccharomyces cerevisiae. Mol. Cell. Biol. **16:** 4189–4198.

Moazed, D., 2001 Common themes in mechanisms of gene silencing. Mol. Cell **8:** 489–498.

Moazed, D., and D. Johnson, 1996 A deubiquitinating enzyme interacts with SIR4 and regulates silencing in S. cerevisiae. Cell **86:** 667–677.

Monson, E. K., D. de Bruin and V. A. Zakian, 1997 The yeast Cac1 protein is required for the stable inheritance of transcriptionally repressed chromatin at telomeres. Proc. Natl. Acad. Sci. USA **94:** 13081–13086.

Moore, C. W., 1989 Cleavage of cellular and extracellular Saccharomyces cerevisiae DNA by bleomycin and phleomycin. Cancer Res. **49:** 6935–6940.

Moore, C. W., J. McKoy, M. Dardalhon, D. Davermann, M. Martinez *et al.*, 2000 DNA damage-inducible and RAD52-independent repair of DNA double-strand breaks in *Saccharomyces cerevisiae*. Genetics **154:** 1085–1099.

Ohba, R., D. J. Steger, J. E. Brownell, C. A. Mizzen, R. G. Cook *et al.*, 1999 A novel H2A/H4 nucleosomal histone acetyltransferase in Tetrahymena thermophila. Mol. Cell. Biol. **19:** 2061–2068.

Park, Y., and A. J. Lustig, 2000 Telomere structure regulates the heritability of repressed subtelomeric chromatin in *Saccharomyces cerevisiae*. Genetics **154:** 587–598.

Pokholok, D. K., N. M. Hannett and R. A. Young, 2002 Exchange of RNA polymerase II initiation and elongation factors during gene expression in vivo. Mol. Cell **9:** 799–809.

Porter, S. E., P. W. Greenwell, K. B. Ritchie and T. D. Petes, 1996 The DNA-binding protein Hdf1p (a putative Ku homologue) is required for maintaining normal telomere length in *Saccharomyces cerevisiae*. Nucleic Acids Res. **24:** 582–585.

Recht, J., and M. A. Osley, 1999 Mutations in both the structured domain and N-terminus of histone H2B bypass the requirement for Swi-Snf in yeast. EMBO J. **18:** 229–240.

Recht, J., B. Dunn, A. Raff and M. A. Osley, 1996 Functional analysis of histones H2A and H2B in transcriptional repression in Saccharomyces cerevisiae. Mol. Cell. Biol. **16:** 2545–2553.

Redon, C., D. Pilch, E. Rogakou, O. Sedelnikova, K. Newrock *et al.*, 2002 Histone H2A variants H2AX and H2AZ. Curr. Opin. Genet. Dev. **12:** 162–169.

Renauld, H., O. M. Aparicio, P. D. Zierath, B. L. Billington, S. K. Chhablani *et al.*, 1993 Silent domains are assembled continuously from the telomere and are defined by promoter distance and strength, and by SIR3 dosage. Genes Dev. **7:** 1133–1145.

Roy, A., F. Exinger and R. Losson, 1990 cis- and trans-acting regulatory elements of the yeast URA3 promoter. Mol. Cell. Biol. **10:** 5257–5270.

Santisteban, M. S., T. Kalashnikova and M. M. Smith, 2000 Histone H2A.Z regulates transcription and is partially redundant with nucleosome remodeling complexes. Cell **103:** 411–422.

Sekinger, E. A., and D. S. Gross, 2001 Silenced chromatin is permissive to activator binding and PIC recruitment. Cell **105:** 403–414.

Sharp, J. A., E. T. Fouts, D. C. Krawitz and P. D. Kaufman, 2001 Yeast histone deposition protein Asf1p requires Hir proteins and PCNA for heterochromatic silencing. Curr. Biol. **11:** 463–473.

Sherwood, P. W., and M. A. Osley, 1991 Histone regulatory (hir) mutations suppress delta insertion alleles in *Saccharomyces cerevisiae*. Genetics **128:** 729–738.

Sherwood, P. W., S. V. Tsang and M. A. Osley, 1993 Characterization of HIR1 and HIR2, two genes required for regulation of histone gene transcription in Saccharomyces cerevisiae. Mol. Cell. Biol. **13:** 28–38.

Suka, N., Y. Suka, A. A. Carmen, J. Wu and M. Grunstein, 2001 Highly specific antibodies determine histone acetylation site usage in yeast heterochromatin and euchromatin. Mol. Cell **8:** 473–479.

Swanson, M. S., E. A. Malone and F. Winston, 1991 SPT5, an essential gene important for normal transcription in Saccharomyces cerevisiae, encodes an acidic nuclear protein with a carboxy-terminal repeat. Mol. Cell. Biol. **11:** 3009–3019.

Thompson, J. S., X. Ling and M. Grunstein, 1994 Histone H3 amino terminus is required for telomeric and silent mating locus repression in yeast. Nature **369:** 245–247.

Venditti, S., M. A. Vega-Palas and E. Di Mauro, 1999 Heterochromatin organization of a natural yeast telomere. Recruitment of Sir3p through interaction with histone H4 N terminus is required for the establishment of repressive structures. J. Biol. Chem. **274:** 1928–1933.

Vogelauer, M., J. Wu, N. Suka and M. Grunstein, 2000 Global histone acetylation and deacetylation in yeast. Nature **408:** 495–498.

Ward, I. M., and J. Chen, 2001 Histone H2AX is phosphorylated in an ATR-dependent manner in response to replicational stress. J. Biol. Chem. **276:** 47759–47762.

White, D. A., N. D. Belyaev and B. M. Turner, 1999 Preparation of site-specific antibodies to acetylated histones. Methods **19:** 417–424.

Winzeler, E. A., D. D. Shoemaker, A. Astromoff, H. Liang, K. Anderson *et al.*, 1999 Functional characterization of the S. cerevisiae genome by gene deletion and parallel analysis. Science **285:** 901–906.

Wittmeyer, J., L. Joss and T. Formosa, 1999 Spt16 and Pob3 of Saccharomyces cerevisiae form an essential, abundant heterodimer that is nuclear, chromatin-associated, and copurifies with DNA polymerase alpha. Biochemistry **38:** 8961–8971.

Wright, J. H., D. E. Gottschling and V. A. Zakian, 1992 Saccharomyces telomeres assume a non-nucleosomal chromatin structure. Genes Dev. **6:** 197–210.

Yamaguchi, Y., T. Narita, N. Inukai, T. Wada and H. Handa, 2001 SPT genes: key players in the regulation of transcription, chromatin structure and other cellular processes. J. Biochem. **129:** 185–191.

Communicating editor: F. Winston